Supplementary material for: *Sensitivity analysis and scaling of tsunamis generated by granular flows at Stromboli volcano: A numerical modeling approach*

S1 Locations of the virtual gauges

Table S1 lists the precise geographical coordinates (WGS-84 UTM Zone 33N) and the local water depths of the 11 virtual gauges used to record the simulated tsunami waveforms around Stromboli island.

N	Name	X [m]	Y [m]	Depth [m a.s.l.]
0	Punta dei Corvi	516,789	4294442	−54
1	–	518,348	4295986	−46
2	–	516,788	4294437	−54
3	Punta Labronzo	518,427	4296006	−33
4	–	514,822	4299420	−1,474
5	–	514,871	4298650	−1,338
6	–	517,871	4295280	−98
7	–	521,152	4295020	−2
8	–	520,599	4295436	−9
9	Stromboli	521,020	4294513	−12
10	Ginostra	516,350	4293057	−15

Table S1. Coordinates (WGS-84 UTM Zone 33N) and local water depths of the 11 virtual gauges used to record the simulated tsunami waveforms.

S2 Sensitivity analysis

Details of the global sensitivity analysis described in Sections 3.2, 4.2, and 5.1 of the main article are reported in the following. In particular, Figs. S1–S12 show first order (blue) and total (orange) Sobol indices (with their confidence interval) as obtained by using the `scipy.stats.sobol_indices` implementation provided by the SciPy library.

Figures S1–S3 and Tables S2–S4 are for the reference dataset; Figures S4–S6 and Tables S5–S7 are for the dataset extended with δ; Figures S7–S9 and Tables S8–S10 are for the dataset extended with m_f; Figures S10–S12 and Tables S11–S13 are for the dataset extended with D.

Figures S1, S4, S7, S10 and Tables S2, S5, S8, S11 represent the analysis performed on the whole dataset; Figures S2, S5, S8, and S11 and Tables S3, S6, S9, and S12 refer to the dataset limited to subaerial scenarios; Figures S3, S6, S9, and S12 and Tables S4, S7, S10, and S13 refer to the dataset limited to submarine scenarios.

The analysis is performed independently for each gauge. Subsequently, an average across all gauges is performed. Values and confidence intervals of the resultant indices are reported in Figures S1–S12 and Tables S2–S13.

In these figures and tables, for each parameter k, first-order indices are S_k, while total indices are S_{T_k}. Along with these indices, the degree of non-additive sensitivity of each parameter is reported through $\Delta_k \equiv S_{T_k} - S_k$. It is the difference between the total and first-order indices of the k-th parameter and measures how strongly the k-th parameter is involved in non-additive effects. More generally, the quantity $1 - \sum_k S_k$ represents the fraction of output variance explained by all non-additive contributions. Likewise, the quantity $\sum_k S_{T_k} - 1$ also reflects the presence of non-additive

effects, although higher-order terms contribute to it with a different weight. In the present application, however, the quantities

$$\frac{1}{2}\sum_k \Delta_k, \qquad 1-\sum_k S_k, \qquad \sum_k S_{T_k} - 1$$

are found to be nearly identical, indicating that non-additive effects are dominated by pairwise contributions and that higher-order terms are negligible. In Tables S2–S13, in addition to S_{T_k}, Δ_k and S_T are reported the total Sobol indices normalized to 1, defined as:

$$s_k \equiv \frac{S_{T_k}}{S_T} \quad \text{for the reference dataset}\,,$$
$$s_k^j \equiv \frac{S_{T_k}}{S_T} \quad \text{for the extended dataset } j \in [\delta, m_f, D]\,.$$

Table S14 compares the normalized primary indices s_i ($i \in [V,\, q,\, \rho]$), obtained from the reference dataset, with those obtained from the extended datasets, namely

$$z_i^j = \frac{s_i^j}{1-s_j^j}\,, \quad \text{with } i \in [V, q, \rho] \text{ and } j \in [\delta, m_f, D]\,.$$

For each primary parameter i, the standard deviation between s_i and z_i^j ($j \in [\delta, m_f, D]$) is reported as σ_i. The same procedure has been applied to the datasets limited to subaerial and submarine scenarios in Tables S15 and S16, respectively. Across all cases, low values of σ_i highlight the robustness of the methodology, enabling the quantification of the Sobol indices across all parameters with data obtained from extended datasets. More specifically, low values of σ_i indicate that the normalized total sensitivities of the primary parameters are only weakly affected by the inclusion of one additional secondary parameter, thereby supporting the use of the reduced datasets to infer the overall hierarchy of sensitivities.

Figure S13 and Table S17 summarize the results of the sensitivity analysis, reporting the normalized total Sobol indices Z_k, across all gauges and their average. These indices provide a synthetic measure of the relative sensitivity of the output to each parameter, while the full first-order and total Sobol indices reported in the preceding figures and tables retain the detailed information on additive and non-additive contributions.

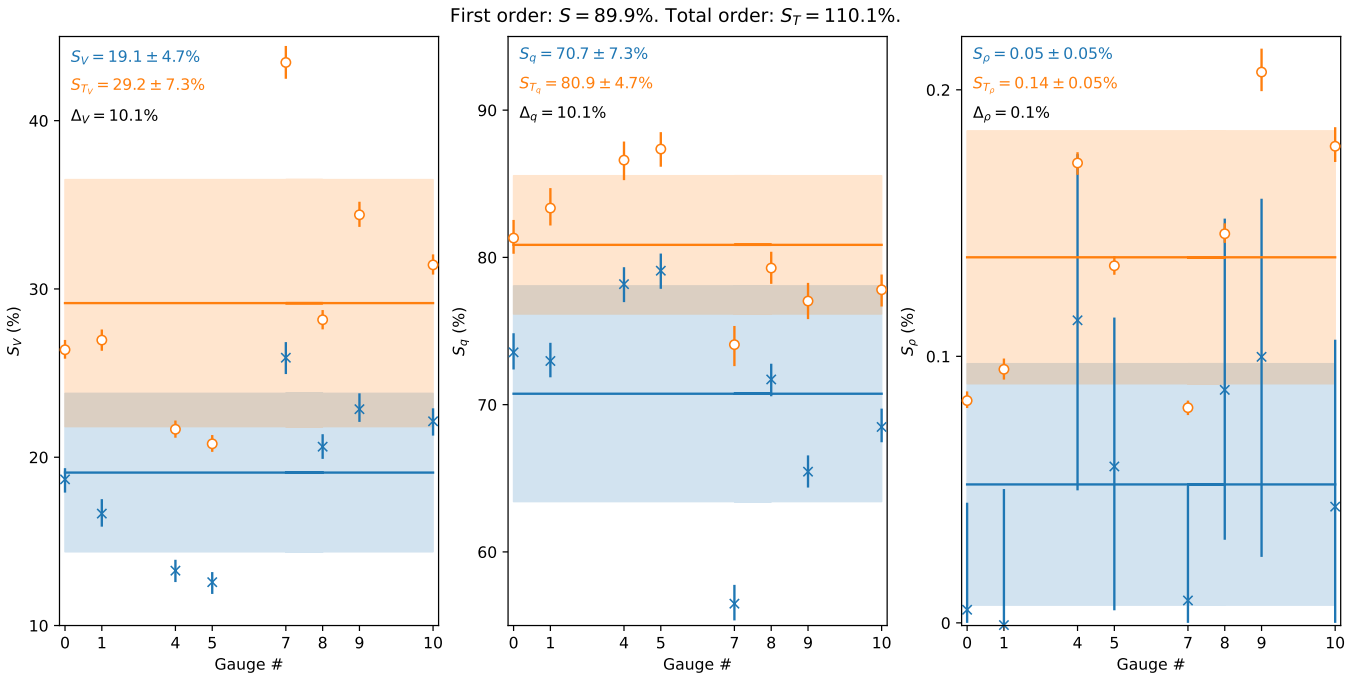

Figure S1. Sobol first-order (blue) and total (orange) indices across gauges, for the reference dataset. Horizontal lines represent the average and shaded areas the confidence interval, with values reported in legend. For each parameter, the degree of interactions with the others is quantified by $\Delta_k \equiv S_{T_k} - S_k$, with $k \in [V, q, \rho]$. Left panel is for V, central for q, and right for ρ

Gauge #	S_{T_V}	Δ_V	S_{T_q}	Δ_q	S_{T_ρ}	Δ_ρ	S_T	S_{T_V}/S_T	S_{T_q}/S_T	S_{T_ρ}/S_T
0	26.4	7.7	81.3	7.8	0.1	0.1	107.8	24.5	75.4	0.1
1	27.0	10.3	83.3	10.4	0.1	0.1	110.4	24.4	75.5	0.1
4	21.7	8.4	86.6	8.4	0.2	0.1	108.4	20.0	79.9	0.2
5	20.8	8.2	87.4	8.3	0.1	0.1	108.3	19.2	80.7	0.1
7	43.5	17.6	74.1	17.6	0.1	0.1	117.6	37.0	63.0	0.1
8	28.2	7.5	79.3	7.5	0.1	0.1	107.6	26.2	73.7	0.1
9	34.4	11.5	77.0	11.6	0.2	0.1	111.6	30.8	69.0	0.2
10	31.4	9.3	77.8	9.3	0.2	0.1	109.4	28.7	71.1	0.2
Avg	29.2	10.1	80.9	10.1	0.1	0.1	110.1	26.5	73.4	0.1

Table S2. Sobol total indices S_{T_k}, interaction parameter Δ_k, and normalized total indices s_k, for the reference dataset ($k \in [V, q, \rho]$). Last row is the average across all gauges

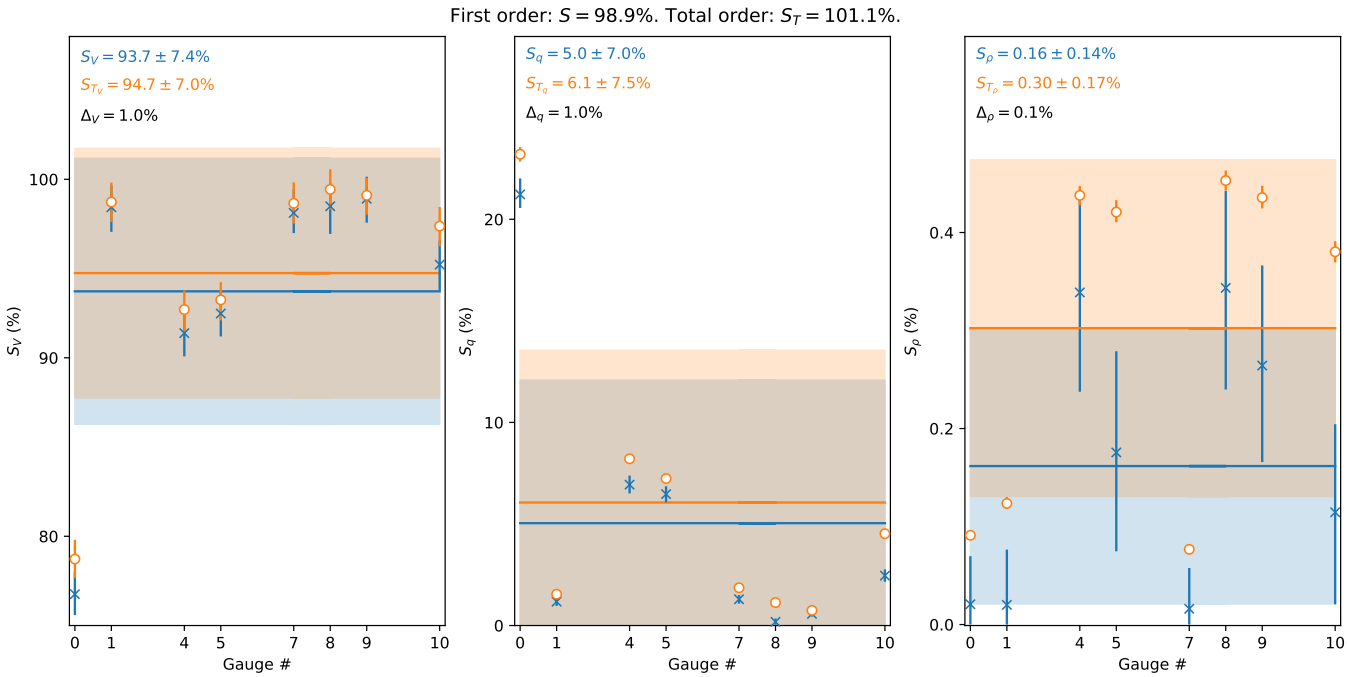

Figure S2. Sobol first-order (blue) and total (orange) indices across gauges, for the reference dataset limited to **subaerial** scenarios. Horizontal lines represent the average and shaded areas the confidence interval, with values reported in legend. For each parameter, the degree of interactions with the others is quantified by $\Delta_k \equiv S_{T_k} - S_k$, with $k \in [V, q, \rho]$. Left panel is for V, central for q, and right for ρ

Gauge #	S_{T_V}	Δ_V	S_{T_q}	Δ_q	S_{T_ρ}	Δ_ρ	S_T	S_{T_V}/S_T	S_{T_q}/S_T	S_{T_ρ}/S_T
0	78.7	2.0	23.2	2.0	0.1	0.1	102.0	77.2	22.7	0.1
1	98.7	0.3	1.5	0.4	0.1	0.1	100.4	98.3	1.5	0.1
4	92.7	1.3	8.2	1.3	0.4	0.1	101.3	91.5	8.1	0.4
5	93.2	0.8	7.2	0.8	0.4	0.2	100.9	92.4	7.2	0.4
7	98.7	0.5	1.9	0.6	0.1	0.1	100.6	98.1	1.8	0.1
8	99.4	0.9	1.1	1.0	0.5	0.1	101.0	98.4	1.1	0.4
9	99.1	0.2	0.7	0.2	0.4	0.2	100.3	98.8	0.7	0.4
10	97.4	2.2	4.5	2.1	0.4	0.3	102.3	95.2	4.4	0.4
Avg	94.7	1.0	6.1	1.0	0.3	0.1	101.1	93.7	6.0	0.3

Table S3. Sobol total indices S_{T_k}, interaction parameter Δ_k, and normalized total indices s_k, for the reference dataset ($k \in [V, q, \rho]$) limited to **subaerial** scenarios. Last row is the average across all gauges

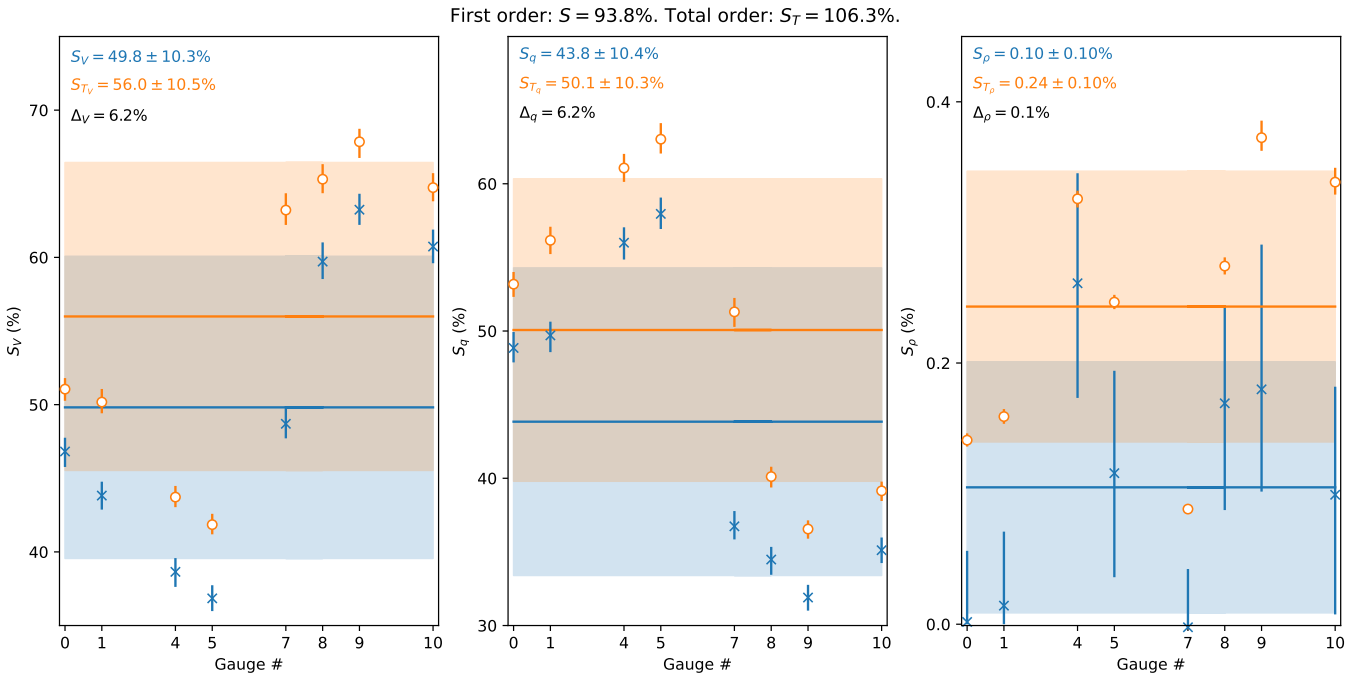

Figure S3. Sobol first-order (blue) and total (orange) indices across gauges, for the reference dataset limited to **submarine** scenarios. Horizontal lines represent the average and shaded areas the confidence interval, with values reported in legend. For each parameter, the degree of interactions with the others is quantified by $\Delta_k \equiv S_{T_k} - S_k$, with $k \in [V, q, \rho]$. Left panel is for V, central for q, and right for ρ

Gauge #	S_{T_V}	Δ_V	S_{T_q}	Δ_q	S_{T_ρ}	Δ_ρ	S_T	S_{T_V}/S_T	S_{T_q}/S_T	S_{T_ρ}/S_T
0	51.1	4.2	53.2	4.3	0.1	0.1	104.4	48.9	51.0	0.1
1	50.2	6.3	56.2	6.5	0.2	0.1	106.5	47.1	52.7	0.1
4	43.7	5.1	61.1	5.1	0.3	0.1	105.1	41.6	58.1	0.3
5	41.9	5.0	63.0	5.1	0.2	0.1	105.1	39.8	60.0	0.2
7	63.2	14.5	51.3	14.6	0.1	0.1	114.6	55.2	44.8	0.1
8	65.3	5.6	40.1	5.6	0.3	0.1	105.7	61.8	37.9	0.3
9	67.8	4.6	36.6	4.7	0.4	0.2	104.8	64.8	34.9	0.4
10	64.7	4.0	39.1	4.0	0.3	0.2	104.2	62.1	37.6	0.3
Avg	56.0	6.2	50.1	6.2	0.2	0.1	106.3	52.7	47.1	0.2

Table S4. Sobol total indices S_{T_k}, interaction parameter Δ_k, and normalized total indices s_k, for the reference dataset ($k \in [V, q, \rho]$) limited to **submarine** scenarios. Last row is the average across all gauges

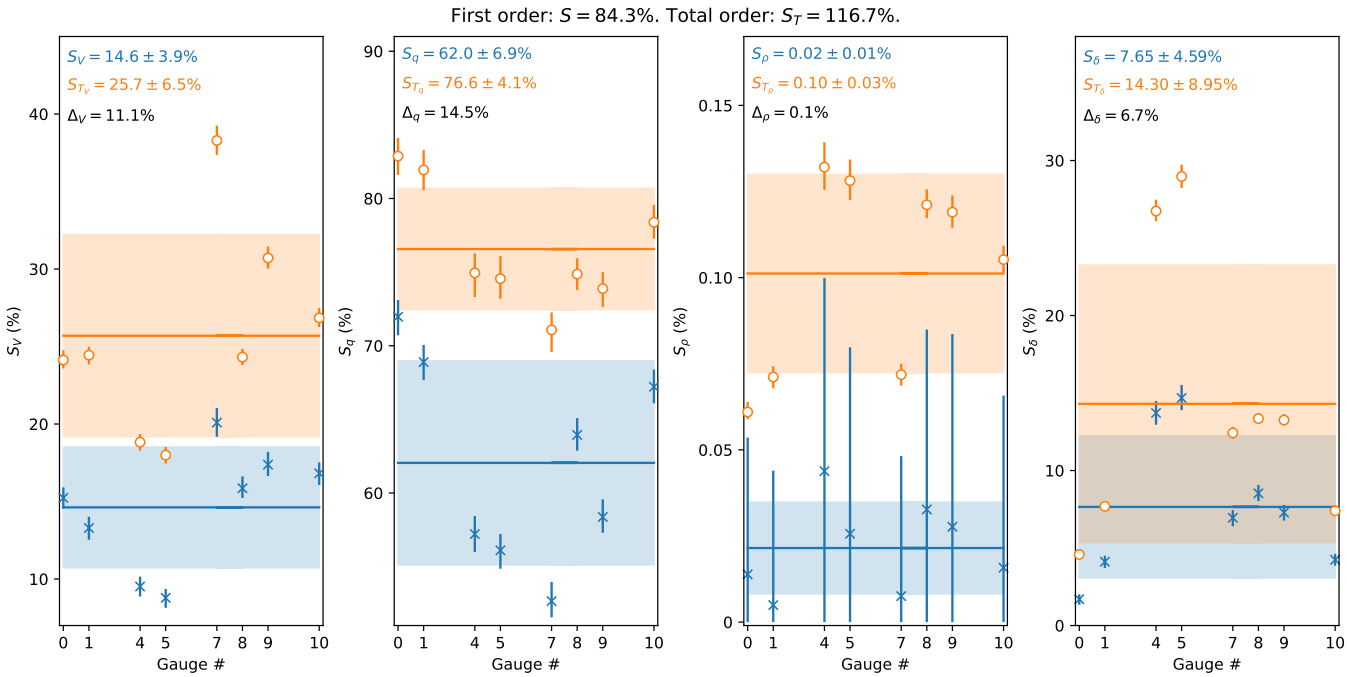

Figure S4. Sobol first-order (blue) and total (orange) indices across gauges, for the dataset extended with δ. Horizontal lines represent the average and shaded areas the confidence interval, with values reported in legend. For each parameter, the degree of interactions with the others is quantified by $\Delta_k \equiv S_{T_k} - S_k$, with $k \in [V, q, \rho, \delta]$. From left to right, panels are for V, q, ρ, δ, respectively

Gauge #	S_{T_V}	Δ_V	S_{T_q}	Δ_q	S_{T_ρ}	Δ_ρ	S_{T_δ}	Δ_δ	S_T	S_{T_V}/S_T	S_{T_q}/S_T	S_{T_ρ}/S_T	S_{T_δ}/S_T
0	24.1	8.9	82.9	10.9	0.1	0.0	4.6	2.9	111.6	21.6	74.2	0.1	4.1
1	24.4	11.1	81.9	13.1	0.1	0.1	7.7	3.6	114.1	21.4	71.8	0.1	6.7
4	18.8	9.3	74.9	17.7	0.1	0.1	26.7	13.0	120.6	15.6	62.1	0.1	22.2
5	18.0	9.2	74.6	18.5	0.1	0.1	29.0	14.3	121.6	14.8	61.3	0.1	23.8
7	38.3	18.2	71.1	18.4	0.1	0.1	12.4	5.5	121.9	31.4	58.3	0.1	10.2
8	24.3	8.5	74.9	10.9	0.1	0.1	13.4	4.8	112.7	21.6	66.5	0.1	11.9
9	30.7	13.3	73.9	15.5	0.1	0.1	13.3	6.0	118.0	26.0	62.6	0.1	11.2
10	26.9	10.0	78.4	11.2	0.1	0.1	7.4	3.2	112.7	23.8	69.5	0.1	6.6
Avg	25.7	11.1	76.6	14.5	0.1	0.1	14.3	6.7	116.7	22.0	65.6	0.1	12.3

Table S5. Sobol total indices S_{T_k}, interaction parameter Δ_k, and normalized total indices s_k, for the extended dataset with $k \in [V, q, \rho, \delta]$. Last row is the average across all gauges

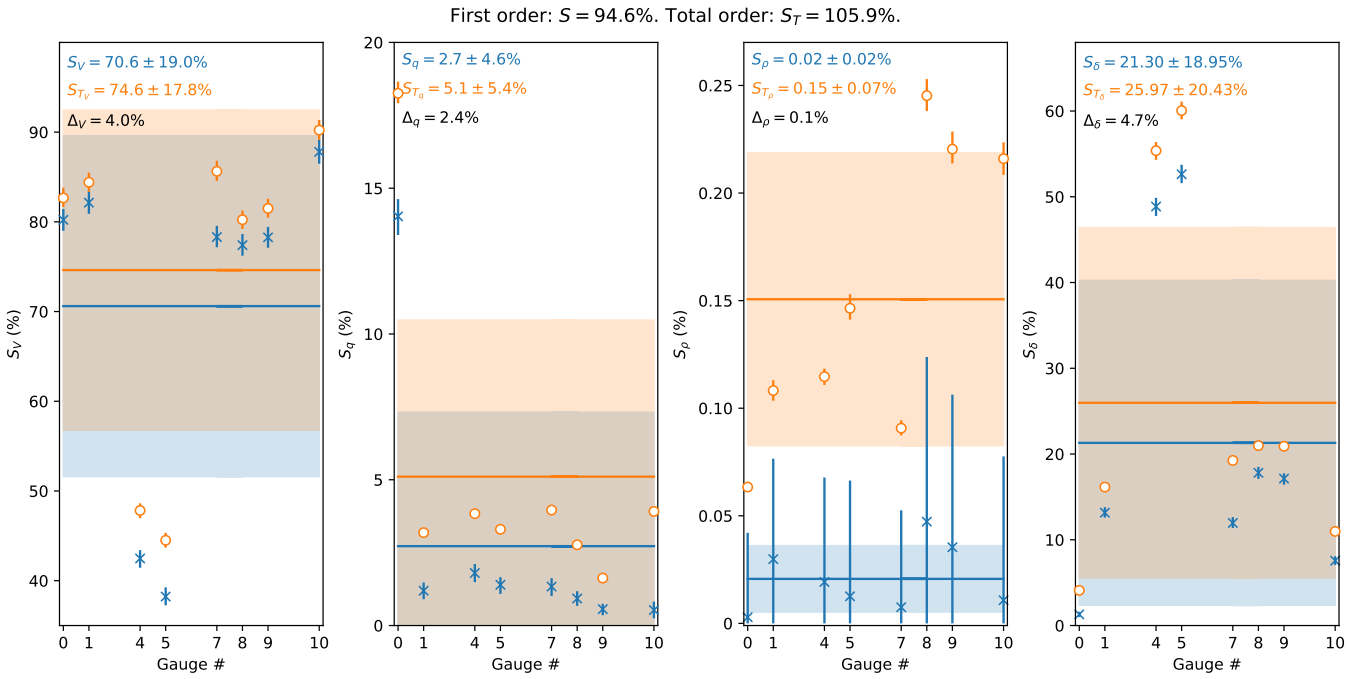

Figure S5. Sobol first-order (blue) and total (orange) indices across gauges, for the dataset extended with δ and limited to **subaerial** scenarios. Horizontal lines represent the average and shaded areas the confidence interval, with values reported in legend. For each parameter, the degree of interactions with the others is quantified by $\Delta_k \equiv S_{T_k} - S_k$, with $k \in [V, q, \rho, \delta]$. From left to right, panels are for V, q, ρ, δ, respectively

Gauge #	S_{T_V}	Δ_V	S_{T_q}	Δ_q	S_{T_ρ}	Δ_ρ	S_{T_δ}	Δ_δ	S_T	S_{T_V}/S_T	S_{T_q}/S_T	S_{T_ρ}/S_T	S_{T_δ}/S_T
0	82.7	2.4	18.3	4.2	0.1	0.1	4.1	2.8	105.1	78.7	17.4	0.1	3.9
1	84.4	2.3	3.2	2.0	0.1	0.1	16.1	3.0	103.8	81.3	3.1	0.1	15.5
4	47.8	5.4	3.8	2.0	0.1	0.1	55.4	6.5	107.2	44.6	3.6	0.1	51.7
5	44.5	6.3	3.3	1.9	0.1	0.1	60.1	7.4	108.0	41.2	3.1	0.1	55.6
7	85.6	7.3	4.0	2.6	0.1	0.1	19.3	7.3	108.9	78.6	3.6	0.1	17.7
8	80.2	2.8	2.8	1.8	0.2	0.2	21.0	3.2	104.2	77.0	2.7	0.2	20.1
9	81.5	3.2	1.6	1.1	0.2	0.2	20.9	3.8	104.2	78.2	1.6	0.2	20.1
10	90.2	2.4	3.9	3.4	0.2	0.2	11.0	3.4	105.3	85.7	3.7	0.2	10.4
Avg	74.6	4.0	5.1	2.4	0.2	0.1	26.0	4.7	105.9	70.5	4.8	0.1	24.5

Table S6. Sobol total indices S_{T_k}, interaction parameter Δ_k, and normalized total indices s_k, for the extended dataset with $k \in [V, q, \rho, \delta]$, limited to **subaerial** scenarios. Last row is the average across all gauges

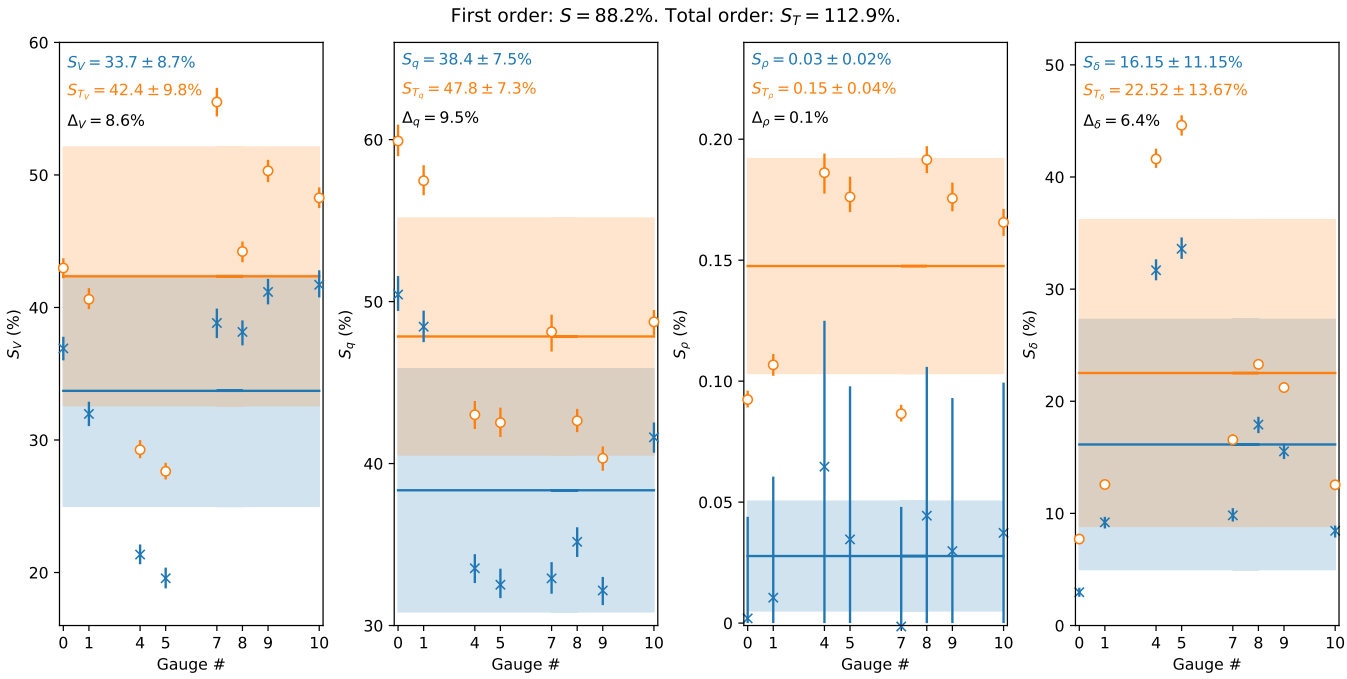

Figure S6. Sobol first-order (blue) and total (orange) indices across gauges, for the dataset extended with δ and limited to **submarine** scenarios. Horizontal lines represent the average and shaded areas the confidence interval, with values reported in legend. For each parameter, the degree of interactions with the others is quantified by $\Delta_k \equiv S_{T_k} - S_k$, with $k \in [V, q, \rho, \delta]$. From left to right, panels are for V, q, ρ, δ, respectively

Gauge #	S_{T_V}	Δ_V	S_{T_q}	Δ_q	S_{T_ρ}	Δ_ρ	S_{T_δ}	Δ_δ	S_T	S_{T_V}/S_T	S_{T_q}/S_T	S_{T_ρ}/S_T	S_{T_δ}/S_T
0	43.0	6.1	59.9	9.5	0.1	0.1	7.7	4.7	110.7	38.8	54.1	0.1	7.0
1	40.6	8.6	57.5	9.0	0.1	0.1	12.6	3.4	110.8	36.7	51.9	0.1	11.4
4	29.3	7.9	43.0	9.5	0.2	0.1	41.6	9.9	114.1	25.7	37.7	0.2	36.5
5	27.6	8.1	42.5	10.0	0.2	0.1	44.6	11.0	114.9	24.0	37.0	0.2	38.8
7	55.5	16.7	48.1	15.2	0.1	0.1	16.6	6.7	120.3	46.1	40.0	0.1	13.8
8	44.2	6.1	42.6	7.5	0.2	0.1	23.3	5.4	110.4	40.1	38.6	0.2	21.1
9	50.3	9.1	40.3	8.2	0.2	0.1	21.2	5.7	112.0	44.9	36.0	0.2	18.9
10	48.3	6.6	48.7	7.1	0.2	0.1	12.5	4.1	109.7	44.0	44.4	0.2	11.4
Avg	42.4	8.6	47.8	9.5	0.1	0.1	22.5	6.4	112.9	37.5	42.4	0.1	20.0

Table S7. Sobol total indices S_{T_k}, interaction parameter Δ_k, and normalized total indices s_k, for the extended dataset with $k \in [V, q, \rho, \delta]$, limited to **submarine** scenarios. Last row is the average across all gauges

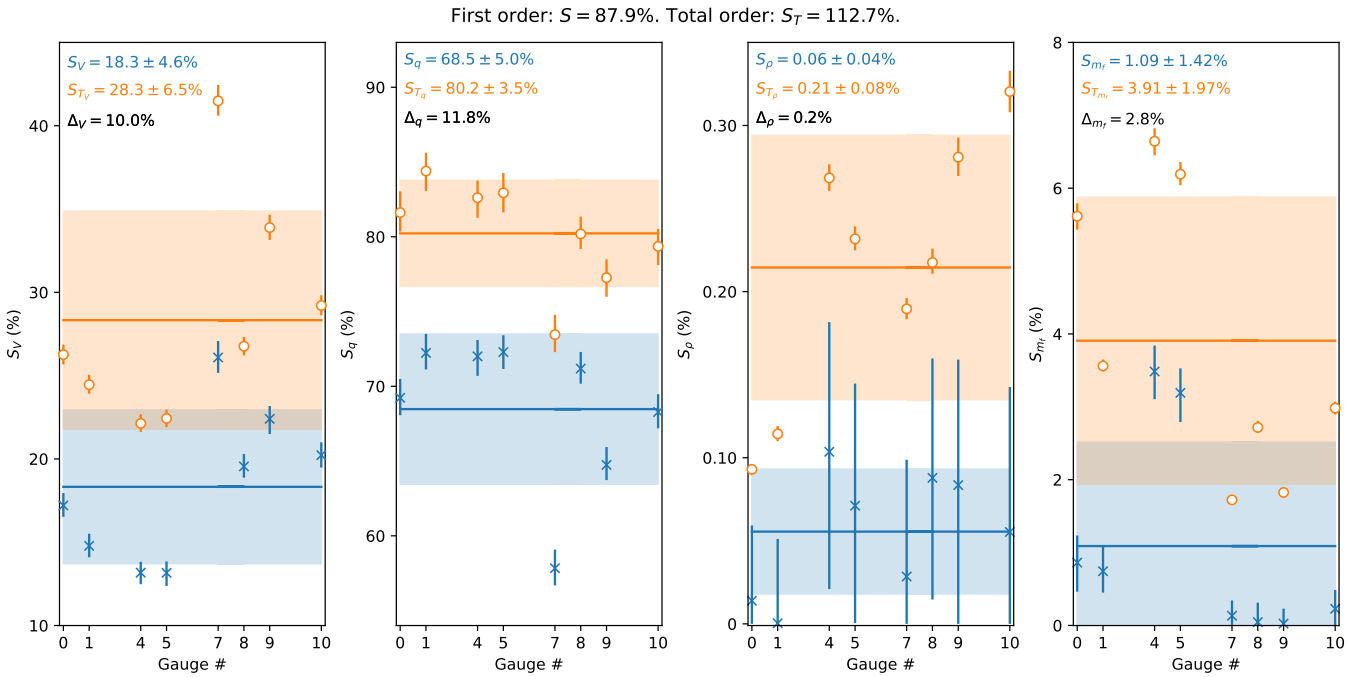

Figure S7. Sobol first-order (blue) and total (orange) indices across gauges, for the dataset extended with m_f. Horizontal lines represent the average and shaded areas the confidence interval, with values reported in legend. For each parameter, the degree of interactions with the others is quantified by $\Delta_k \equiv S_{T_k} - S_k$, with $k \in [V, q, \rho, m_f]$. From left to right, panels are for V, q, ρ, m_f, respectively

Gauge #	S_{T_V}	Δ_V	S_{T_q}	Δ_q	S_{T_ρ}	Δ_ρ	$S_{T_{m_f}}$	Δ_{m_f}	S_T	S_{T_V}/S_T	S_{T_q}/S_T	S_{T_ρ}/S_T	$S_{T_{m_f}}/S_T$
0	26.3	9.1	81.6	12.4	0.1	0.1	5.6	4.8	113.6	23.1	71.9	0.1	4.9
1	24.5	9.7	84.4	12.2	0.1	0.1	3.6	2.8	112.5	21.7	75.0	0.1	3.2
4	22.1	9.0	82.6	10.6	0.3	0.2	6.6	3.2	111.7	19.8	74.0	0.2	6.0
5	22.4	9.3	82.9	10.6	0.2	0.2	6.2	3.0	111.8	20.1	74.2	0.2	5.5
7	41.5	15.4	73.5	15.6	0.2	0.2	1.7	1.6	116.9	35.5	62.9	0.2	1.5
8	26.8	7.2	80.2	9.0	0.2	0.1	2.7	2.7	109.9	24.4	73.0	0.2	2.5
9	33.9	11.5	77.3	12.5	0.3	0.2	1.8	1.8	113.3	29.9	68.2	0.2	1.6
10	29.2	9.0	79.4	11.1	0.3	0.3	3.0	2.8	111.9	26.1	70.9	0.3	2.7
Avg	28.3	10.0	80.2	11.8	0.2	0.2	3.9	2.8	112.7	25.1	71.2	0.2	3.5

Table S8. Sobol total indices S_{T_k}, interaction parameter Δ_k, and normalized total indices s_k, for the extended dataset with $k \in [V, q, \rho, m_f]$. Last row is the average across all gauges

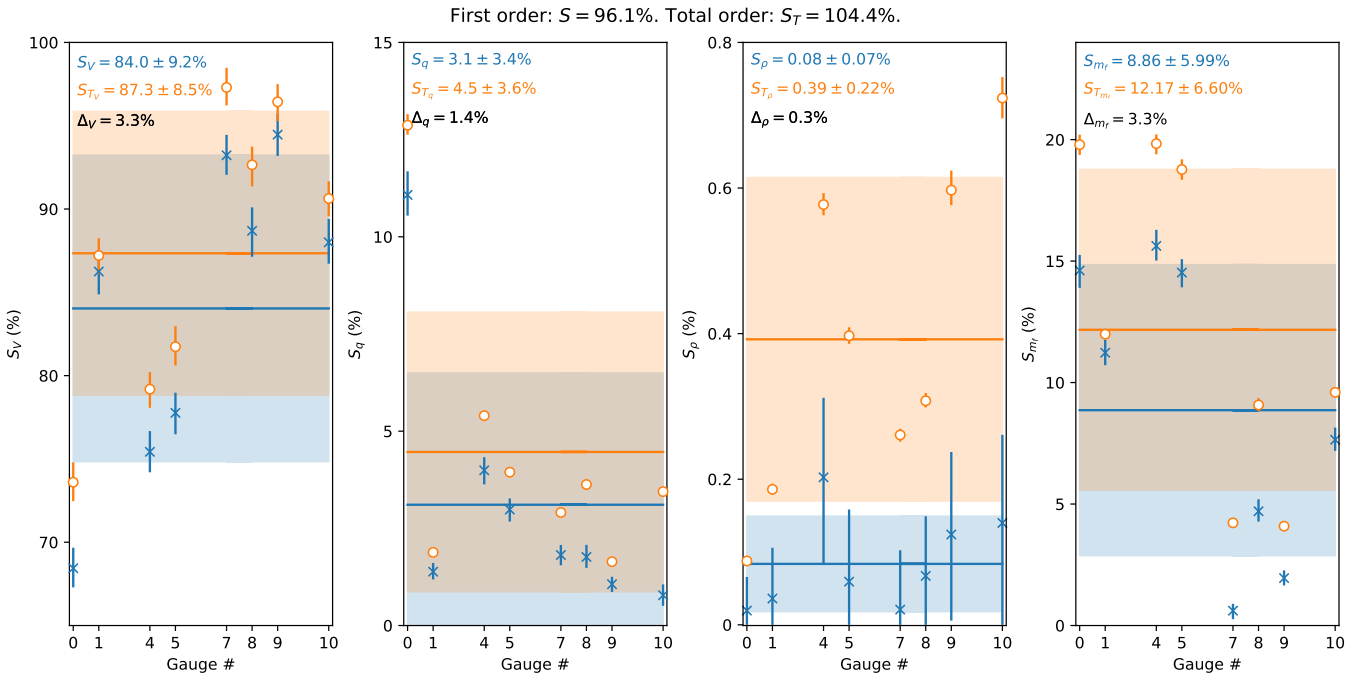

Figure S8. Sobol first-order (blue) and total (orange) indices across gauges, for the dataset extended with m_f and limited to **subaerial** scenarios. Horizontal lines represent the average and shaded areas the confidence interval, with values reported in legend. For each parameter, the degree of interactions with the others is quantified by $\Delta_k \equiv S_{T_k} - S_k$, with $k \in [V, q, \rho, m_f]$. From left to right, panels are for V, q, ρ, m_f, respectively

Gauge #	S_{T_V}	Δ_V	S_{T_q}	Δ_q	S_{T_ρ}	Δ_ρ	$S_{T_{m_f}}$	Δ_{m_f}	S_T	S_{T_V}/S_T	S_{T_q}/S_T	S_{T_ρ}/S_T	$S_{T_{m_f}}/S_T$
0	73.6	5.2	12.9	1.8	0.1	0.1	19.8	5.2	106.4	69.2	12.1	0.1	18.6
1	87.2	1.0	1.9	0.5	0.2	0.2	12.0	0.8	101.3	86.1	1.9	0.2	11.8
4	79.2	3.8	5.4	1.4	0.6	0.4	19.8	4.2	105.0	75.4	5.1	0.5	18.9
5	81.7	4.0	3.9	1.0	0.4	0.3	18.8	4.2	104.8	78.0	3.8	0.4	17.9
7	97.3	4.1	2.9	1.1	0.3	0.2	4.2	3.6	104.7	92.9	2.8	0.2	4.0
8	92.7	4.0	3.6	1.9	0.3	0.2	9.1	4.4	105.7	87.7	3.4	0.3	8.6
9	96.4	2.0	1.6	0.6	0.6	0.5	4.1	2.1	102.8	93.8	1.6	0.6	4.0
10	90.6	2.6	3.4	2.7	0.7	0.6	9.6	2.0	104.4	86.8	3.3	0.7	9.2
Avg	87.3	3.3	4.5	1.4	0.4	0.3	12.2	3.3	104.4	83.7	4.3	0.4	11.7

Table S9. Sobol total indices S_{T_k}, interaction parameter Δ_k, and normalized total indices s_k, for the extended dataset with $k \in [V, q, \rho, m_f]$, limited to **subaerial** scenarios. Last row is the average across all gauges

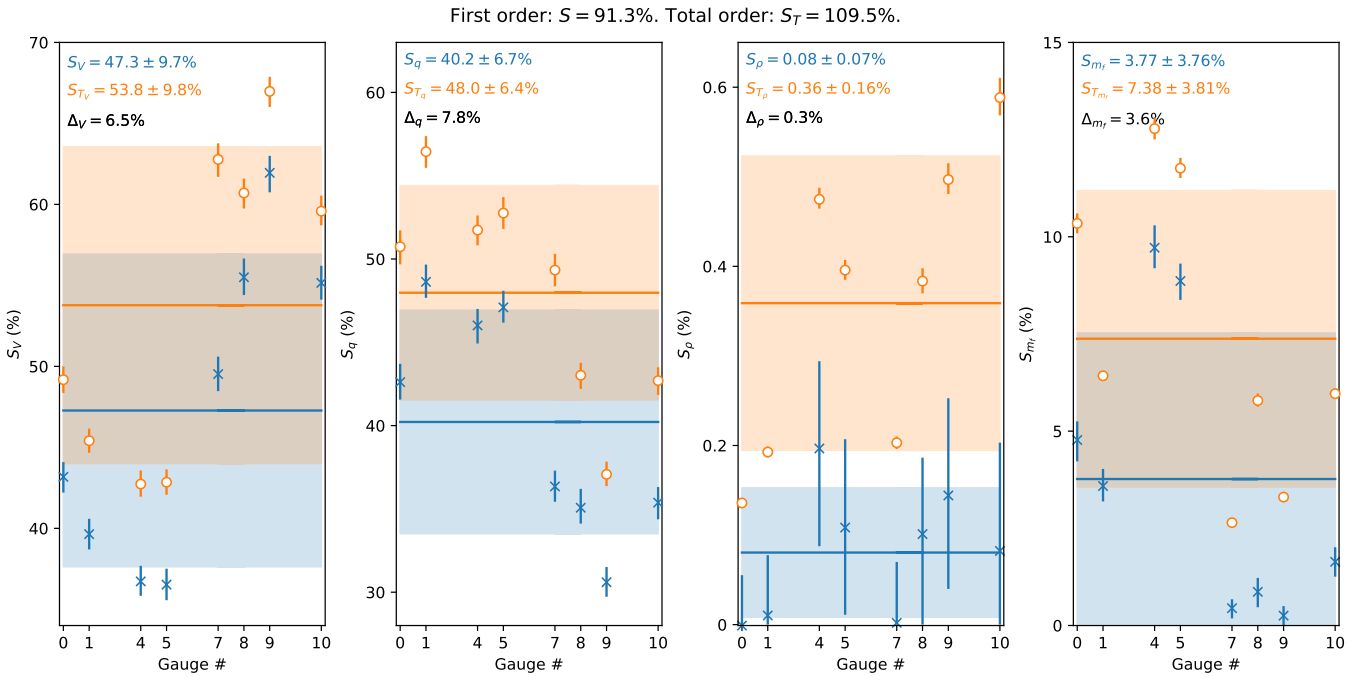

Figure S9. Sobol first-order (blue) and total (orange) indices across gauges, for the dataset extended with m_f and limited to **submarine** scenarios. Horizontal lines represent the average and shaded areas the confidence interval, with values reported in legend. For each parameter, the degree of interactions with the others is quantified by $\Delta_k \equiv S_{T_k} - S_k$, with $k \in [V, q, \rho, m_f]$. From left to right, panels are for V, q, ρ, m_f, respectively

Gauge #	S_{T_V}	Δ_V	S_{T_q}	Δ_q	S_{T_ρ}	Δ_ρ	$S_{T_{m_f}}$	Δ_{m_f}	S_T	S_{T_V}/S_T	S_{T_q}/S_T	S_{T_ρ}/S_T	$S_{T_{m_f}}/S_T$
0	49.2	6.0	50.7	8.1	0.1	0.1	10.3	5.6	110.4	44.5	46.0	0.1	9.4
1	45.4	5.8	56.4	7.8	0.2	0.2	6.4	2.8	108.5	41.9	52.0	0.2	5.9
4	42.7	6.0	51.7	5.7	0.5	0.3	12.8	3.1	107.7	39.7	48.0	0.4	11.9
5	42.8	6.3	52.8	5.7	0.4	0.3	11.8	2.9	107.8	39.8	49.0	0.4	10.9
7	62.8	13.3	49.3	13.0	0.2	0.2	2.6	2.2	115.0	54.6	42.9	0.2	2.3
8	60.7	5.2	43.0	8.0	0.4	0.3	5.8	4.9	109.9	55.2	39.1	0.3	5.3
9	67.0	5.0	37.1	6.5	0.5	0.4	3.3	3.1	107.9	62.1	34.4	0.5	3.1
10	59.6	4.4	42.7	7.3	0.6	0.5	6.0	4.3	108.8	54.7	39.2	0.5	5.5
Avg	53.8	6.5	48.0	7.8	0.4	0.3	7.4	3.6	109.5	49.1	43.8	0.3	6.7

Table S10. Sobol total indices S_{T_k}, interaction parameter Δ_k, and normalized total indices s_k, for the extended dataset with $k \in [V, q, \rho, m_f]$, limited to **submarine** scenarios. Last row is the average across all gauges

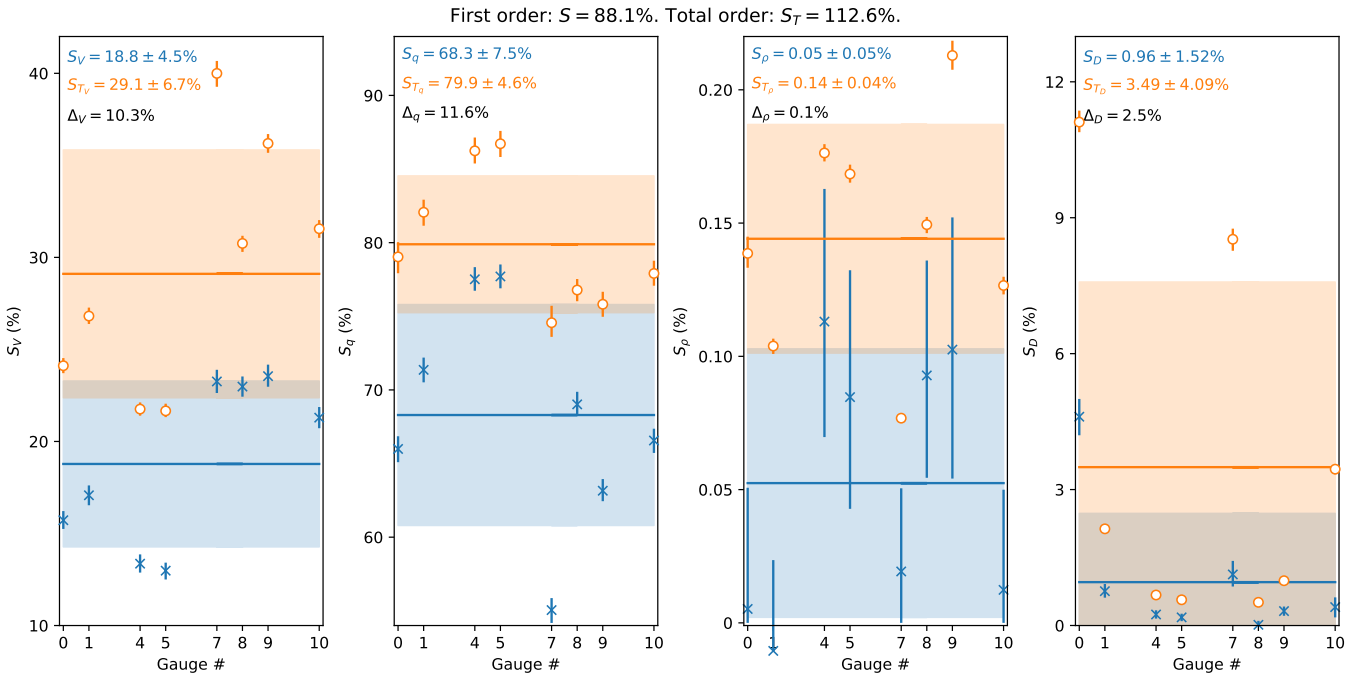

Figure S10. Sobol first-order (blue) and total (orange) indices across gauges, for the dataset extended with D. Horizontal lines represent the average and shaded areas the confidence interval, with values reported in legend. For each parameter, the degree of interactions with the others is quantified by $\Delta_k \equiv S_{T_k} - S_k$, with $k \in [V, q, \rho, D]$. From left to right, panels are for V, q, ρ, D, respectively

Gauge #	S_{T_V}	Δ_V	S_{T_q}	Δ_q	S_{T_ρ}	Δ_ρ	S_{T_D}	Δ_D	S_T	S_{T_V}/S_T	S_{T_q}/S_T	S_{T_ρ}/S_T	S_{T_D}/S_T
0	24.1	8.4	79.0	13.0	0.1	0.1	11.1	6.5	114.4	21.1	69.1	0.1	9.7
1	26.8	9.7	82.1	10.7	0.1	0.1	2.1	1.4	111.1	24.1	73.9	0.1	1.9
4	21.8	8.4	86.2	8.7	0.2	0.1	0.7	0.4	108.8	20.0	79.2	0.2	0.6
5	21.7	8.7	86.7	9.0	0.2	0.1	0.6	0.4	109.1	19.9	79.5	0.2	0.5
7	40.0	16.7	74.6	19.6	0.1	0.0	8.5	7.5	123.2	32.5	60.5	0.1	6.9
8	30.8	7.8	76.8	7.8	0.1	0.1	0.5	0.5	108.2	28.4	71.0	0.1	0.5
9	36.2	12.7	75.8	12.6	0.2	0.1	1.0	0.7	113.2	32.0	67.0	0.2	0.9
10	31.6	10.2	77.9	11.3	0.1	0.1	3.5	3.0	113.1	27.9	68.9	0.1	3.1
Avg	29.1	10.3	79.9	11.6	0.1	0.1	3.5	2.5	112.6	25.8	70.9	0.1	3.1

Table S11. Sobol total indices S_{T_k}, interaction parameter Δ_k, and normalized total indices s_k, for the extended dataset with $k \in [V, q, \rho, D]$. Last row is the average across all gauges

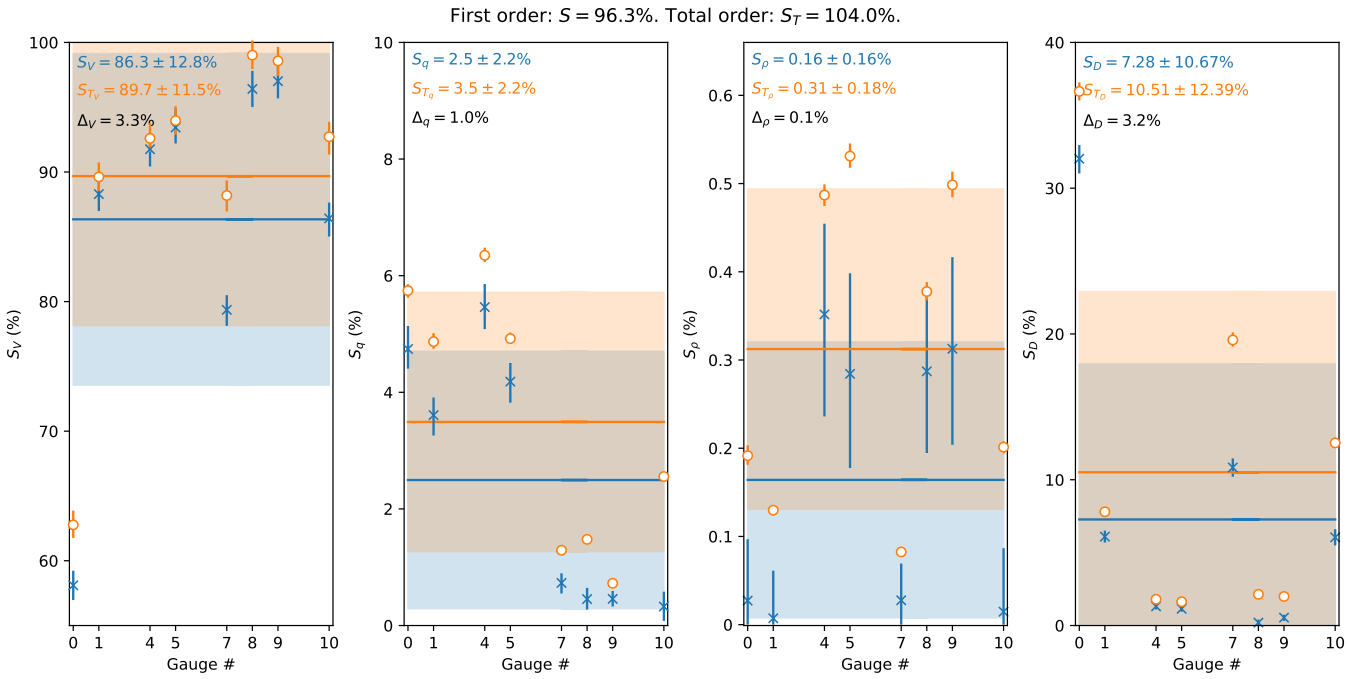

Figure S11. Sobol first-order (blue) and total (orange) indices across gauges, for the dataset extended with D and limited to **subaerial** scenarios. Horizontal lines represent the average and shaded areas the confidence interval, with values reported in legend. For each parameter, the degree of interactions with the others is quantified by $\Delta_k \equiv S_{T_k} - S_k$, with $k \in [V, q, \rho, D]$. From left to right, panels are for V, q, ρ, D, respectively

Gauge #	S_{T_V}	Δ_V	S_{T_q}	Δ_q	S_{T_ρ}	Δ_ρ	S_{T_D}	Δ_D	S_T	S_{T_V}/S_T	S_{T_q}/S_T	S_{T_ρ}/S_T	S_{T_D}/S_T
0	62.8	4.7	5.7	1.0	0.2	0.2	36.6	4.6	105.3	59.6	5.5	0.2	34.8
1	89.6	1.3	4.9	1.3	0.1	0.1	7.8	1.7	102.4	87.5	4.8	0.1	7.6
4	92.6	0.8	6.3	0.9	0.5	0.1	1.8	0.5	101.2	91.5	6.3	0.5	1.8
5	94.0	0.5	4.9	0.7	0.5	0.2	1.6	0.5	101.0	93.0	4.9	0.5	1.6
7	88.2	8.8	1.3	0.6	0.1	0.1	19.6	8.7	109.1	80.8	1.2	0.1	17.9
8	99.0	2.6	1.5	1.0	0.4	0.1	2.1	1.9	103.0	96.1	1.4	0.4	2.1
9	98.6	1.6	0.7	0.3	0.5	0.2	2.0	1.5	101.8	96.8	0.7	0.5	2.0
10	92.7	6.3	2.6	2.2	0.2	0.2	12.5	6.5	108.0	85.8	2.4	0.2	11.6
Avg	89.7	3.3	3.5	1.0	0.3	0.1	10.5	3.2	104.0	86.2	3.4	0.3	10.1

Table S12. Sobol total indices S_{T_k}, interaction parameter Δ_k, and normalized total indices s_k, for the extended dataset with $k \in [V, q, \rho, D]$, limited to **subaerial** scenarios. Last row is the average across all gauges

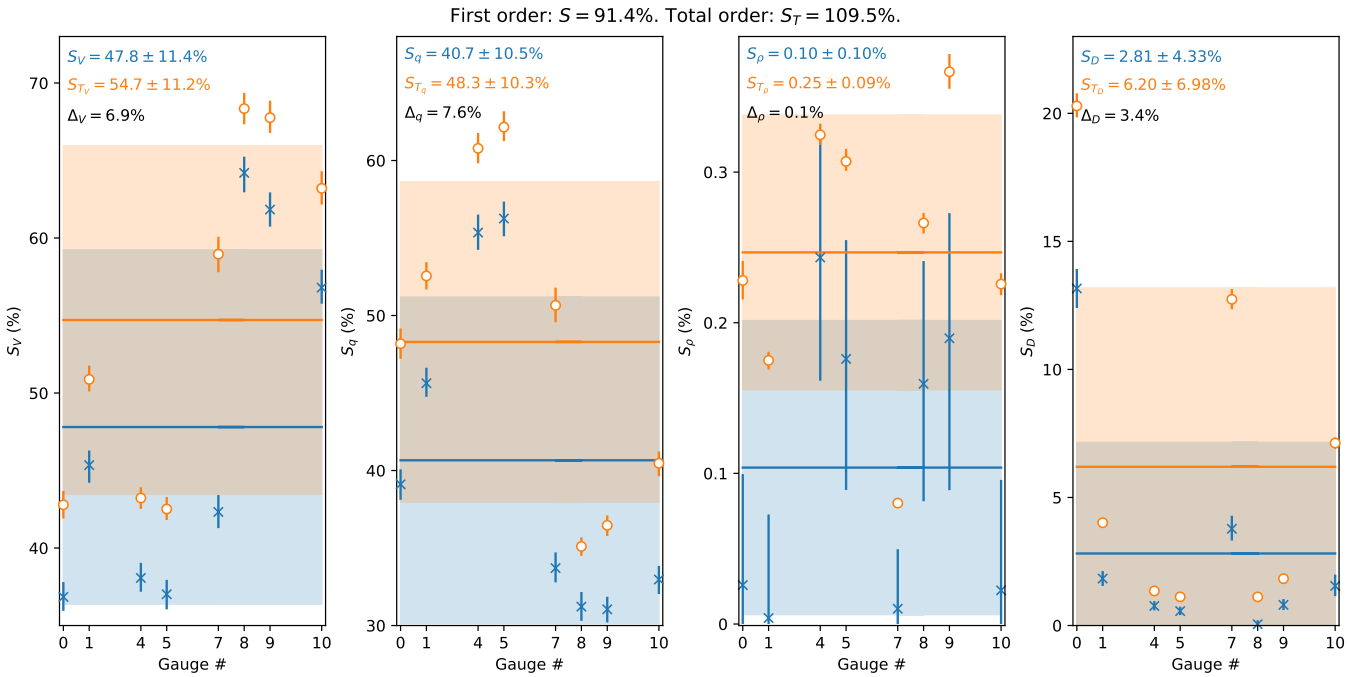

Figure S12. Sobol first-order (blue) and total (orange) indices across gauges, for the dataset extended with D and limited to **submarine** scenarios. Horizontal lines represent the average and shaded areas the confidence interval, with values reported in legend. For each parameter, the degree of interactions with the others is quantified by $\Delta_k \equiv S_{T_k} - S_k$, with $k \in [V, q, \rho, D]$. From left to right, panels are for V, q, ρ, D, respectively

Gauge #	S_{T_V}	Δ_V	S_{T_q}	Δ_q	S_{T_ρ}	Δ_ρ	S_{T_D}	Δ_D	S_T	S_{T_V}/S_T	S_{T_q}/S_T	S_{T_ρ}/S_T	S_{T_D}/S_T
0	42.8	5.9	48.2	9.1	0.2	0.2	20.3	7.1	111.5	38.4	43.2	0.2	18.2
1	50.9	5.5	52.6	6.9	0.2	0.2	4.0	2.2	107.6	47.3	48.8	0.2	3.7
4	43.2	5.2	60.8	5.4	0.3	0.1	1.3	0.6	105.7	40.9	57.5	0.3	1.3
5	42.5	5.5	62.2	5.9	0.3	0.1	1.1	0.6	106.1	40.1	58.6	0.3	1.1
7	59.0	16.6	50.7	16.9	0.1	0.1	12.7	9.0	122.4	48.2	41.4	0.1	10.4
8	68.3	4.1	35.1	3.9	0.3	0.1	1.1	1.1	104.8	65.2	33.5	0.3	1.1
9	67.8	5.9	36.5	5.4	0.4	0.2	1.8	1.0	106.4	63.7	34.3	0.3	1.7
10	63.2	6.4	40.5	7.5	0.2	0.2	7.1	5.6	111.0	56.9	36.5	0.2	6.4
Avg	54.7	6.9	48.3	7.6	0.2	0.1	6.2	3.4	109.5	50.0	44.1	0.2	5.7

Table S13. Sobol total indices S_{T_k}, interaction parameter Δ_k, and normalized total indices s_k, for the extended dataset with $k \in [V, q, \rho, D]$, limited to **submarine** scenarios. Last row is the average across all gauges

Gauge #	s_V	$\frac{s_V}{1-s_\delta}$	$\frac{s_V}{1-s_{m_f}}$	$\frac{s_V}{1-s_D}$	σ_V	s_q	$\frac{s_q}{1-s_\delta}$	$\frac{s_q}{1-s_{m_f}}$	$\frac{s_q}{1-s_D}$	σ_q	s_ρ	$\frac{s_\rho}{1-s_\delta}$	$\frac{s_\rho}{1-s_{m_f}}$	$\frac{s_\rho}{1-s_D}$	σ_ρ
0	24.5	22.5	24.3	23.3	0.8	75.4	77.4	75.6	76.5	0.8	0.1	0.1	0.1	0.1	0.0
1	24.4	23.0	22.4	24.6	0.9	75.5	77.0	77.5	75.3	0.9	0.1	0.1	0.1	0.1	0.0
4	20.0	20.0	21.1	20.1	0.4	79.9	79.8	78.7	79.7	0.5	0.2	0.1	0.3	0.2	0.0
5	19.2	19.4	21.2	20.0	0.8	80.7	80.4	78.5	79.9	0.8	0.1	0.1	0.2	0.2	0.0
7	37.0	35.0	36.0	34.9	0.8	63.0	64.9	63.8	65.0	0.9	0.1	0.1	0.2	0.1	0.0
8	26.2	24.5	25.0	28.6	1.6	73.7	75.4	74.8	71.3	1.6	0.1	0.1	0.2	0.1	0.0
9	30.8	29.3	30.4	32.3	1.0	69.0	70.6	69.3	67.6	1.1	0.2	0.1	0.3	0.2	0.0
10	28.7	25.5	26.8	28.8	1.4	71.1	74.4	72.9	71.1	1.4	0.2	0.1	0.3	0.1	0.1
Avg	26.5	25.1	26.0	26.7	0.6	73.4	74.8	73.8	73.2	0.6	0.1	0.1	0.2	0.1	0.0

Table S14. Comparison of the normalized total Sobol indices of the primary parameters, and their standard deviation σ_i, $i \in [V, q, \rho]$, across the 4 datasets. Values are in %

Gauge #	s_V	$\frac{s_V}{1-s_\delta}$	$\frac{s_V}{1-s_{m_f}}$	$\frac{s_V}{1-s_D}$	σ_V	s_q	$\frac{s_q}{1-s_\delta}$	$\frac{s_q}{1-s_{m_f}}$	$\frac{s_q}{1-s_D}$	σ_q	s_ρ	$\frac{s_\rho}{1-s_\delta}$	$\frac{s_\rho}{1-s_{m_f}}$	$\frac{s_\rho}{1-s_D}$	σ_ρ
0	77.2	81.9	85.0	91.4	5.2	22.7	18.1	14.9	8.4	5.2	0.1	0.1	0.1	0.3	0.1
1	98.3	96.2	97.7	94.7	1.4	1.5	3.6	2.1	5.1	1.4	0.1	0.1	0.2	0.1	0.0
4	91.5	92.4	93.0	93.1	0.7	8.1	7.4	6.3	6.4	0.7	0.4	0.2	0.7	0.5	0.2
5	92.4	92.8	95.0	94.5	1.1	7.2	6.9	4.6	4.9	1.1	0.4	0.3	0.5	0.5	0.1
7	98.1	95.5	96.8	98.5	1.2	1.8	4.4	2.9	1.4	1.1	0.1	0.1	0.3	0.1	0.1
8	98.4	96.4	95.9	98.2	1.1	1.1	3.3	3.8	1.5	1.1	0.4	0.3	0.3	0.4	0.1
9	98.8	97.8	97.7	98.8	0.5	0.7	2.0	1.7	0.7	0.5	0.4	0.3	0.6	0.5	0.1
10	95.2	95.6	95.6	97.1	0.7	4.4	4.1	3.6	2.7	0.7	0.4	0.2	0.8	0.2	0.2
Avg	93.7	93.4	94.7	95.9	1.0	6.0	6.4	4.8	3.7	1.0	0.3	0.2	0.4	0.3	0.1

Table S15. As Tab. S14 but limited to **subaerial** scenarios

Gauge #	s_V	$\frac{s_V}{1-s_\delta}$	$\frac{s_V}{1-s_{m_f}}$	$\frac{s_V}{1-s_D}$	σ_V	s_q	$\frac{s_q}{1-s_\delta}$	$\frac{s_q}{1-s_{m_f}}$	$\frac{s_q}{1-s_D}$	σ_q	s_ρ	$\frac{s_\rho}{1-s_\delta}$	$\frac{s_\rho}{1-s_{m_f}}$	$\frac{s_\rho}{1-s_D}$	σ_ρ
0	48.9	41.7	49.2	46.9	3.0	51.0	58.2	50.7	52.8	3.0	0.1	0.1	0.1	0.3	0.1
1	47.1	41.4	44.5	49.1	2.9	52.7	58.5	55.3	50.7	2.9	0.1	0.1	0.2	0.2	0.0
4	41.6	40.4	45.0	41.4	1.7	58.1	59.4	54.5	58.3	1.8	0.3	0.3	0.5	0.3	0.1
5	39.8	39.3	44.6	40.5	2.1	60.0	60.5	55.0	59.2	2.2	0.2	0.3	0.4	0.3	0.1
7	55.2	53.5	55.9	53.7	1.0	44.8	46.4	43.9	46.2	1.0	0.1	0.1	0.2	0.1	0.0
8	61.8	50.8	58.3	65.9	5.5	37.9	49.0	41.3	33.8	5.6	0.3	0.2	0.4	0.3	0.1
9	64.8	55.4	64.1	64.8	4.0	34.9	44.4	35.5	34.9	4.0	0.4	0.2	0.5	0.4	0.1
10	62.1	49.7	57.9	60.8	4.8	37.6	50.2	41.5	39.0	4.9	0.3	0.2	0.6	0.2	0.2
Avg	52.7	46.9	52.7	53.0	2.6	47.1	53.0	47.0	46.8	2.6	0.2	0.2	0.4	0.2	0.1

Table S16. As Tab. S14 but limited to **submarine** scenarios

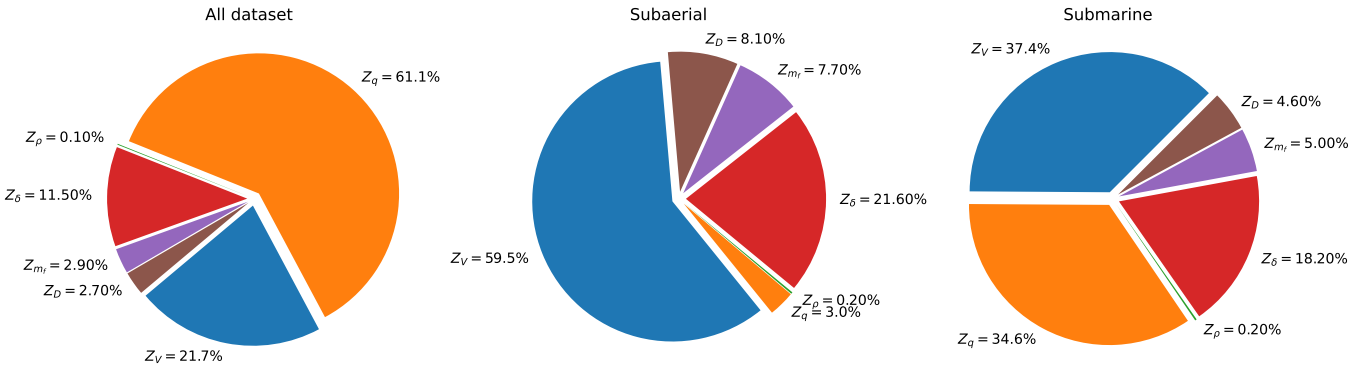

Figure S13. Normalized total Sobol indices for all datasets (left), subaeril (center), and submarine (right)

G.#	Z_V	Z_q	Z_ρ	Z_δ	Z_{m_f}	Z_D	Z_V	Z_q	Z_ρ	Z_δ	Z_{m_f}	Z_D	Z_V	Z_q	Z_ρ	Z_δ	Z_{m_f}	Z_D
0	19.7	63.4	0.1	3.6	4.3	8.9	46.5	8.9	0.1	2.3	12.7	29.6	33.3	38.0	0.1	5.3	7.4	15.9
1	21.0	67.9	0.1	6.4	2.9	1.7	69.1	2.2	0.1	13.1	9.6	5.9	37.0	44.2	0.1	10.4	5.1	3.2
4	15.0	58.7	0.1	21.0	4.7	0.5	39.9	3.0	0.2	46.1	10.0	0.8	24.5	33.4	0.2	33.3	7.8	0.8
5	14.5	58.0	0.1	22.7	4.3	0.4	37.7	2.4	0.2	50.4	8.8	0.7	23.2	33.2	0.2	35.9	6.9	0.6
7	29.7	53.4	0.1	9.4	1.2	6.2	65.9	1.8	0.1	14.5	2.9	14.8	42.0	34.9	0.1	12.3	1.8	8.9
8	22.4	63.4	0.1	11.5	2.2	0.4	71.1	1.8	0.3	18.4	6.9	1.6	44.4	30.4	0.2	20.1	4.2	0.8
9	26.7	60.0	0.2	11.0	1.4	0.8	74.9	1.0	0.3	19.1	3.2	1.5	48.5	29.2	0.3	18.2	2.5	1.4
10	24.3	64.1	0.1	6.2	2.4	2.8	71.1	2.8	0.3	8.6	7.5	9.7	45.9	33.5	0.3	10.3	4.6	5.5
Avg	21.7	61.1	0.1	11.5	2.9	2.7	59.5	3.0	0.2	21.6	7.7	8.1	37.4	34.6	0.2	18.2	5.0	4.6

Table S17. Normalized total Sobol indices for all datasets (left), subaeril (center), and submarine (right)

S3 Integrated waveforms

In addition to the maximum wave height H, we characterized the tsunami impact using integrated metrics that account for the overall temporal evolution and persistence of the positive wave phases. This allows us to verify if the information content of the waveforms and their response to different landslide parameters remain consistent when considering the entire signal duration rather than just the peak amplitude. Specifically, we defined two parameters:

1. w_{0+}: the time-averaged positive wave height computed over a fixed 300 s window starting from the first instance the signal exceeds a threshold $\epsilon = 0.001$ m. Within this window, negative values are set to zero, so that the average reflects the integrated contribution of the positive signal normalized by the window duration.

2. w_{+}: the average height calculated exclusively over the time intervals where the signal is positive ($\geq \epsilon$), isolating the average magnitude of the tsunami positive phases across the record.

An example of these metrics applied to the synthetic waveforms is illustrated in Fig. S14. These metrics provide complementary insights: w_{0+} quantifies the mean impact within a predefined post-trigger timeframe, while w_{+} characterizes the persistent magnitude of the wave crests. To ensure the robustness of the physical trends identified in the main text, we repeated the volume-scaling fits using w_{0+} as the target variable. The results, shown in Figs. S15–S18, demonstrate that the functional dependence on volume (linear for submarine and logarithmic for subaerial sources) as well as the relative variability driven by secondary parameters, are nearly identical to those obtained for H. This consistency confirms that H is a reliable and representative proxy for the overall tsunamigenic potential of the simulated granular flows.

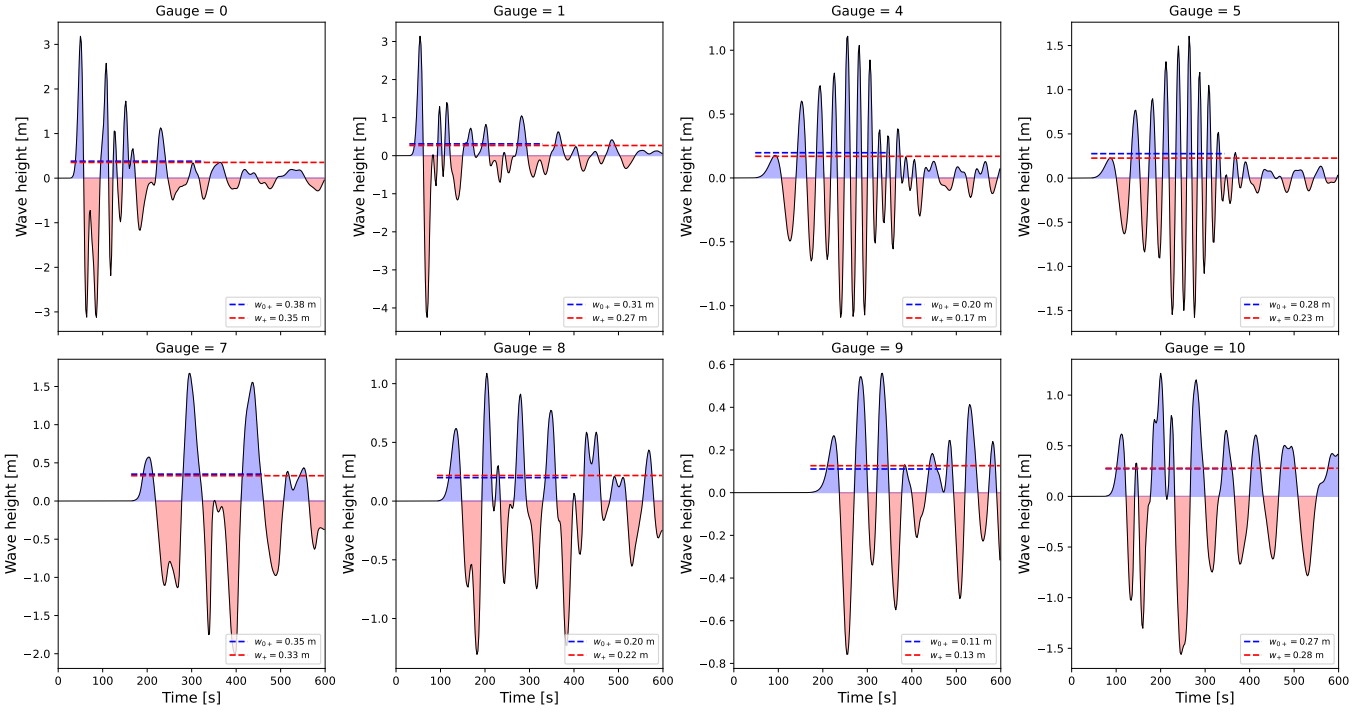

Figure S14. Example of tsunami waveforms recorded at synthetic gauges showing positive (blue) and negative (red) wave phases. The dashed blue line (w_{0+}) represents the time-averaged wave height computed over a fixed 300 s window starting at t_0, the first instance when the signal exceeds a threshold $\epsilon = 0.001$ m. Within this window, negative values are set to zero, so that the average reflects only the integrated contribution of the positive signal, normalized by the window duration. The w_{+} values (dashed red line) correspond to the average wave height calculated only over time intervals where the signal is positive ($\geq \epsilon$), excluding all negative or zero values. These metrics provide complementary insights: w_{0+} quantifies the mean impact within a predefined post-trigger timeframe, while w_{+} isolates the average magnitude of the tsunami positive phases across the entire record. As discussed in the main article, our analysis using these metrics yielded trends nearly identical to those obtained by considering only the maximum wave height

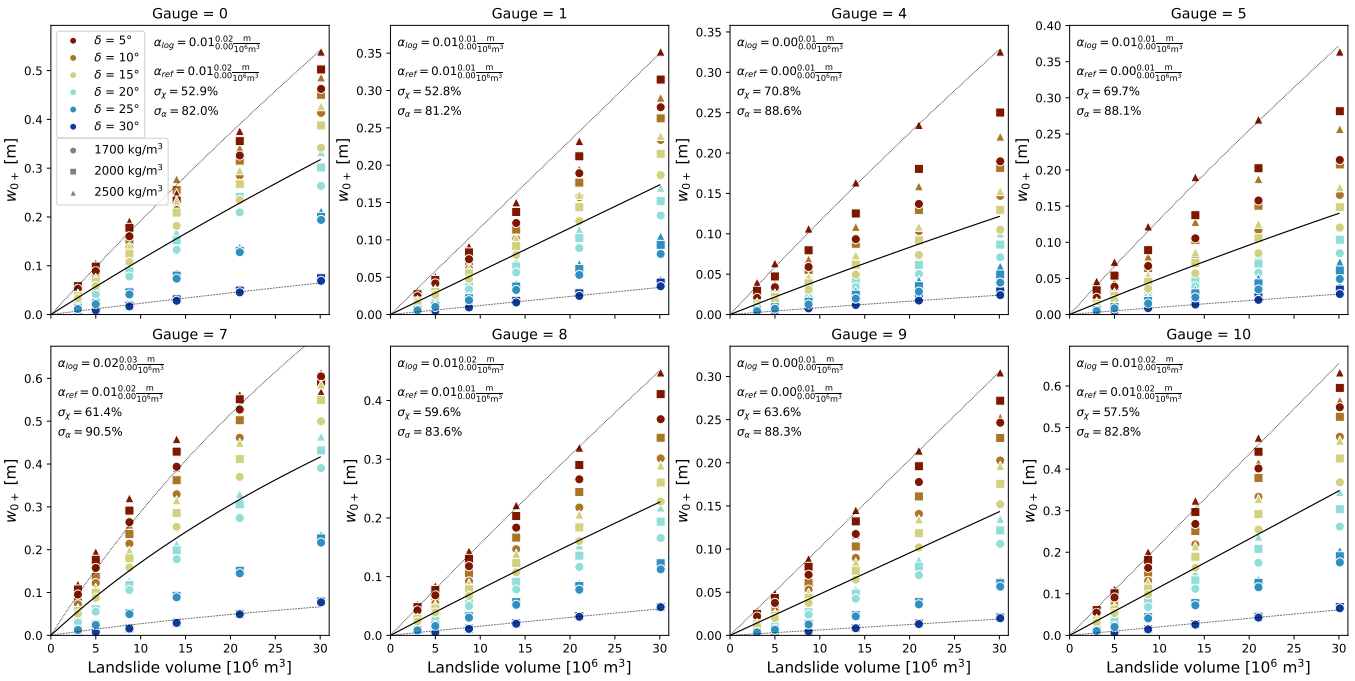

Figure S15. Variability of w_{0+} as a function of the landslide volume for a fixed submarine position (B7, see Fig. S1 in the main article). The wave height is shown for 6 different configurations of friction angles ($\delta_1 = \delta_3 = \{5, 10, 15, 20, 25, 30\}°$, represented by different colors) and 3 different granular mass densities (1700, 2000, and 2500 kg/m^3, represented by symbols: circles, squares, and triangles, respectively). m_f is fixed at 10^{-3} m^{-1}. In each subplot, Eq. 2 (see main article) is used to fit all the reported scenarios (solid line), and the maximum and minimum (dashed lines) among the w_{0+} recorded for each volume across the parameter space. These fits provides best values and variability of $\alpha_{\log}$ and α_{ref} (reported in legend). The normalized fit error σ_χ represents the residual error divided by the number of data points, while σ_α measures the relative difference between the maximum and minimum fitted values, normalized by their sum

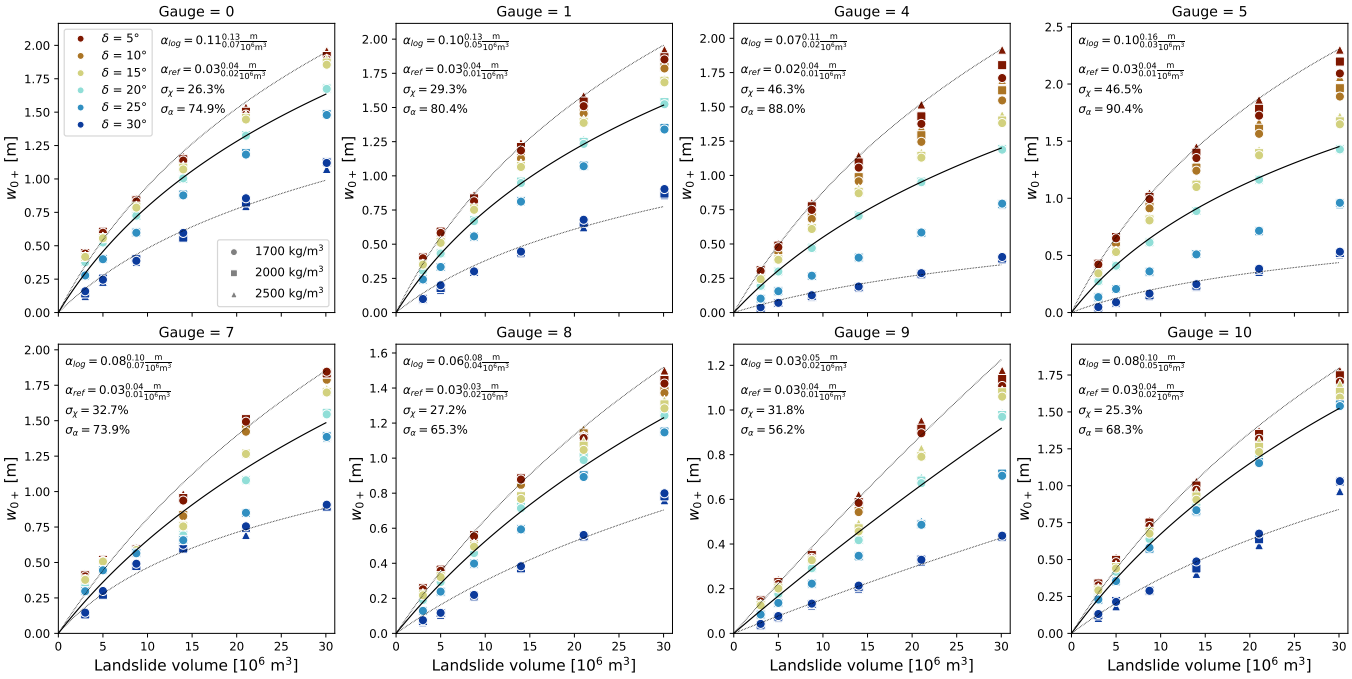

Figure S16. Variability of w_{0+} as a function of the landslide volume for a fixed subaerial starting position (B0, see Fig. S1 in the main article). The results are shown for different friction angles ($\delta_1 = \delta_3 = \{5, 10, 15, 20, 25, 30\}^\circ$; colors) and densities (1700, 2000, and 2500 kg/m^3; symbols) with m_f fixed at 10^{-3} m^{-1}. In each subplot, Eq. 2 (see main article) is used to fit all the reported scenarios (solid line), and the maximum and minimum (dashed lines) among the w_{0+} recorded for each volume across the parameter space. These fits provides best values and variability of $\alpha_{\log}$ and α_{ref} (reported in legend). The normalized fit error σ_χ and the relative difference σ_m are also reported in each subplot. A logarithmic trend is observed for all gauges, causing the slopes of the fit at V = 0 ($\alpha_{\log}$) and V = 30×10^6 m^3 (α_{ref}) to differ

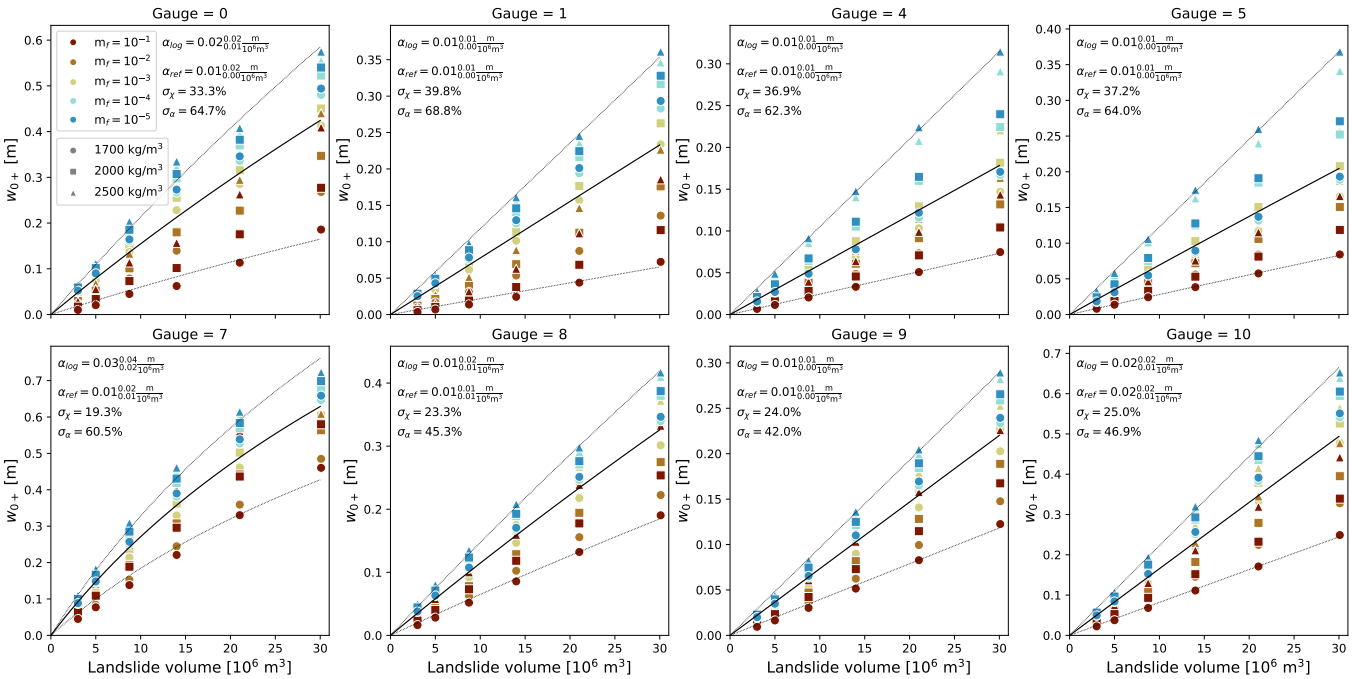

Figure S17. Variability of w_{0+} as a function of the landslide volume for a fixed submarine position (B7, see Fig. S1 in the main article). The wave height is shown for 5 different configurations of m_f ($10^{-1}, 10^{-2}, 10^{-3}, 10^{-4}, 10^{-5}$ m^{-1}, represented by different colors) and 3 different granular mass densities (1700, 2000, and 2500 kg/m^3, represented by symbols: circles, squares, and triangles, respectively). δ_1 is fixed at 15°. In each subplot, Eq. 2 (see main article) is used to fit all the reported scenarios (solid line), and the maximum and minimum (dashed lines) among the w_{0+} recorded for each volume across the parameter space. These fits provides best values and variability of $\alpha_{\log}$ and α_{ref} (reported in legend). The normalized fit error σ_χ represents the residual error divided by the number of data points, while σ_m measures the relative difference between the maximum and minimum fitted values, normalized by their sum. As expected, when the fit is linear, both slopes coincide

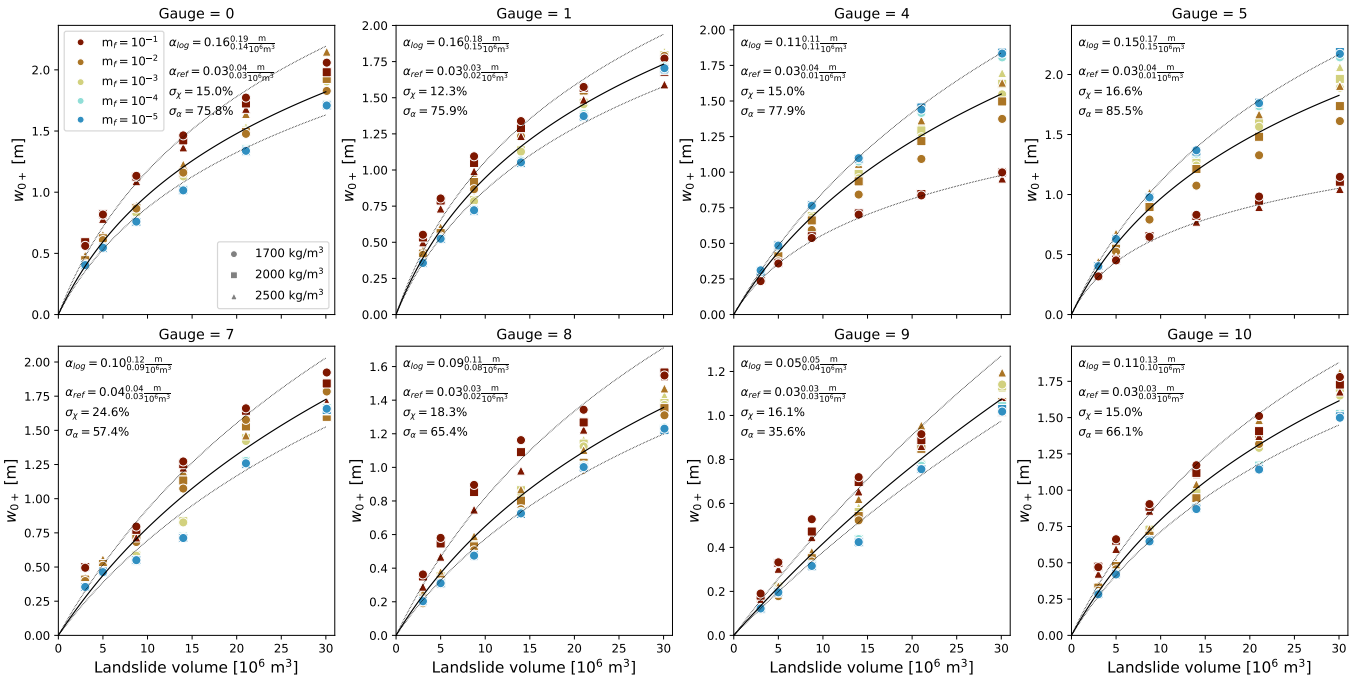

Figure S18. Variability of w_{0+} as a function of the landslide volume for a fixed subaerial starting position (B0, see Fig. S1 in the main article). The results are shown for different m_f ($10^{-1}, 10^{-2}, 10^{-3}, 10^{-4}, 10^{-5}$ m^{-1}; colors) and densities (1700, 2000, and 2500 kg/m^3; symbols) with δ_1 fixed at 15°. In each subplot, Eq. 2 (see main article) is used to fit all the reported scenarios (solid line), and the maximum and minimum (dashed lines) among the w_{0+} recorded for each volume across the parameter space. These fits provides best values and variability of $\alpha_{\log}$ and α_{ref} (reported in legend). The normalized fit error σ_χ and the relative difference σ_m are also reported in each subplot. A logarithmic trend is observed for all gauges, causing the slopes of the fit at V = 0 ($\alpha_{\log}$) and V = 30×10^6 m^3 (α_{ref}) to differ

S4 Wave height dependence on source volume and elevation

Following the methodology described in Section 4.2 of the main article, we analyzed the relationship between maximum wave height H and landslide volume V by calculating best-fitting coefficients for each extended dataset and source elevation. Specifically, for each gauge, the coefficients $\alpha_{\log}$ and α_{ref} (for subaerial sources) and the linear coefficient α_0 (for submarine sources) were computed while allowing slide density ρ and one secondary parameter (δ, m_f, or D) to vary.

Figures S19–S21 show the resulting coefficients as a function of submergence depth s for subaerial scenarios, derived from the datasets extended with friction angles δ, landslide-water coupling m_f, and source azimuth D, respectively. Similarly, Figures S22–S24 report the coefficients for submarine scenarios across the same 3 extended datasets. In these plots, dots represent the best-fit values, while the shaded bars indicate the uncertainty band defined by the maximum and minimum coefficients obtained across all parameter combinations. These detailed analyses provided the basis for the averaged scaling laws and uncertainty ranges presented in the main text (e.g., Figs. 11 and 12 of the main article).

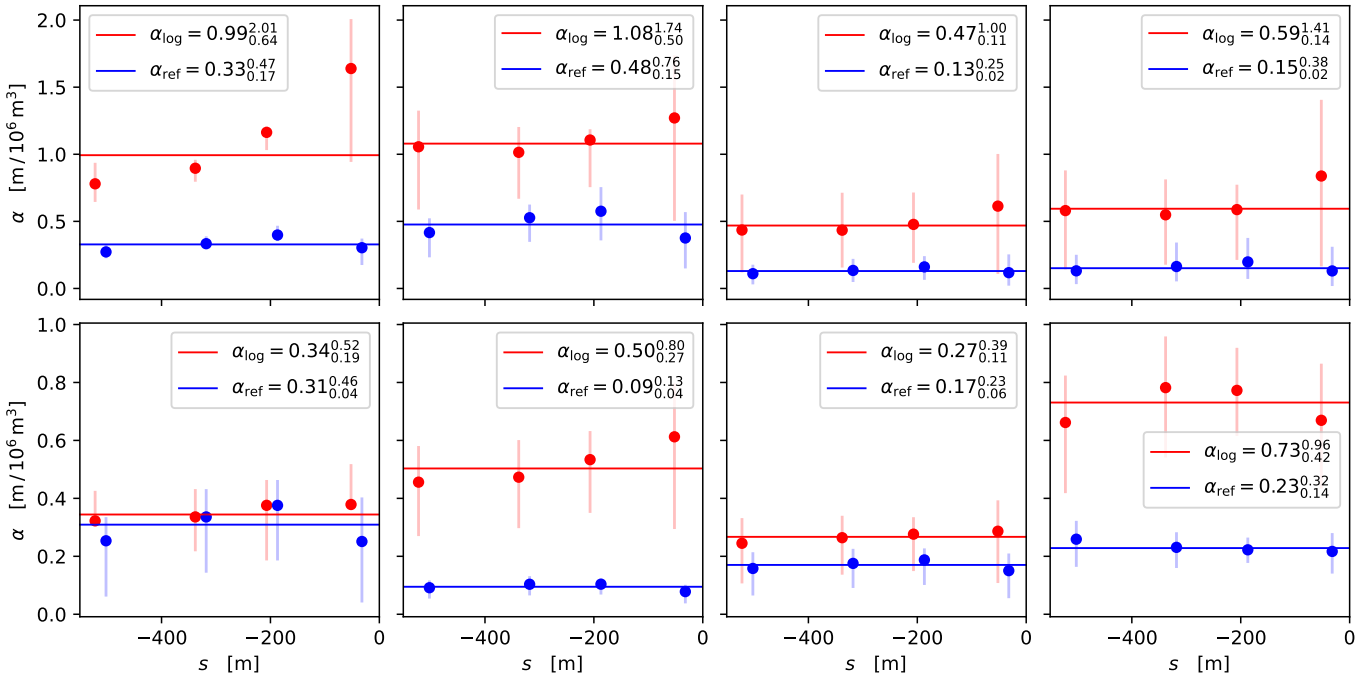

Figure S19. Volume dependence coefficients for subaerial sources as functions of submergence $s = -q$, for the extended dataset with landslide friction angles δ. The analysis includes 6 different configurations of friction angles ($\delta_1 = \delta_3 = \{5, 10, 15, 20, 25, 30\}^\circ$) and 3 different granular mass densities (1700, 2000, and 2500 kg/m^3). m_f is fixed at 10^{-3} m^{-1}, and D corresponds to transect B in Fig. 1 of the main article. Red dots and bars show the best-fit values and corresponding max–min ranges for $\alpha_{\log}$, whereas blue dots and bars show those for α_{ref}. Horizontal lines denote the best-fit constant values obtained from these coefficients and ranges (values reported in the legend)

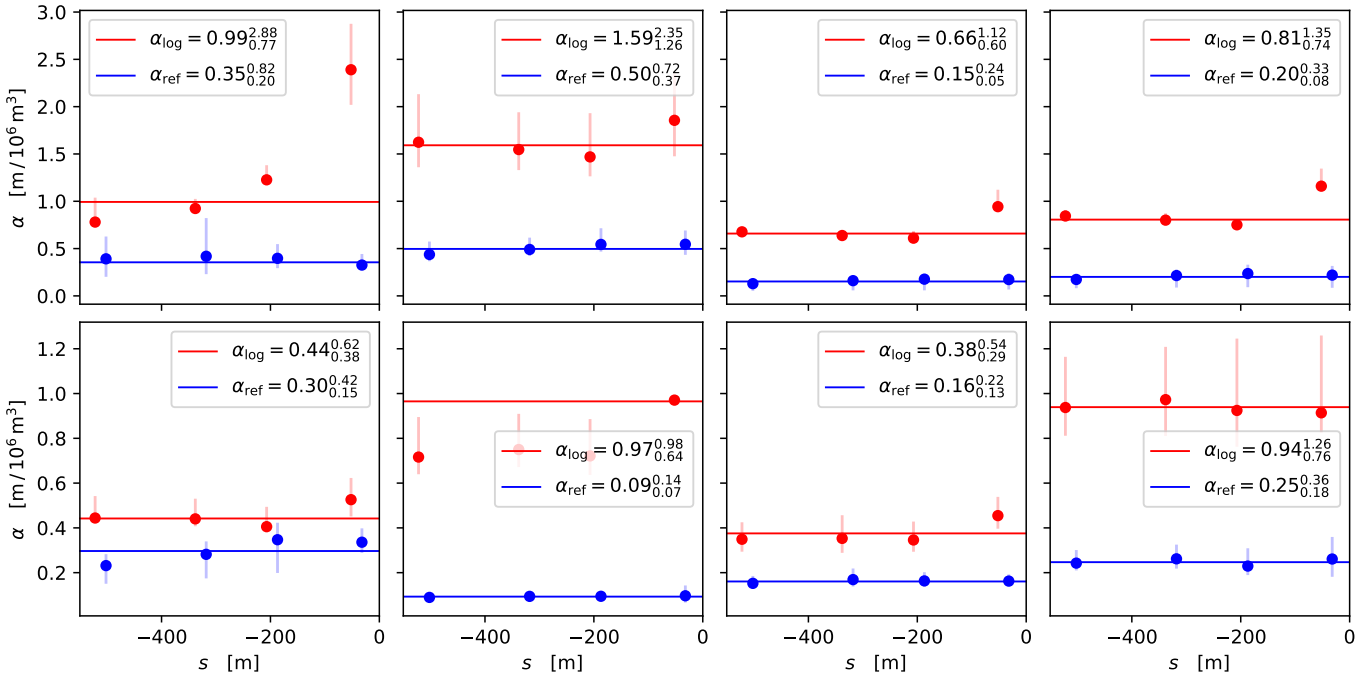

Figure S20. Volume dependence coefficients for subaerial sources as functions of submergence $s = -q$, for the extended dataset with landslide-water coupling m_f. The analysis includes 5 different values of m_f ($10^{-1}, 10^{-2}, 10^{-3}, 10^{-4}, 10^{-5}$ m^{-1}) and 3 different granular mass densities (1700, 2000, and 2500 kg/m^3). δ set is fixed at $[10, 15, 10]^\circ$, and D corresponds to transect B in Fig. 1 of the main article. Red dots and bars show the best-fit values and corresponding max–min ranges for $\alpha_{\log}$, whereas blue dots and bars show those for α_{ref}. Horizontal lines denote the best-fit constant values obtained from these coefficients and ranges (values reported in the legend)

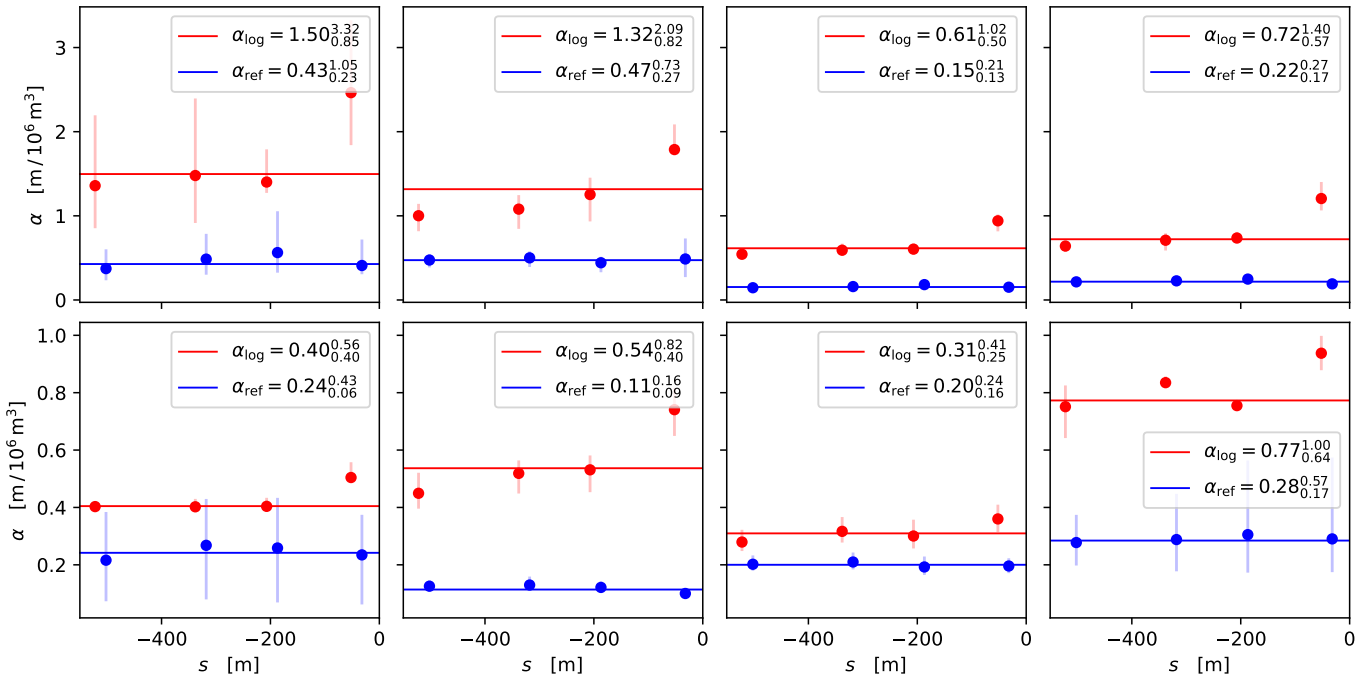

Figure S21. Volume dependence coefficients for subaerial sources as functions of submergence $s = -q$, for the extended dataset with source azimuth D. The analysis includes 3 different source azimuths ($312°, 320, 2°, 327.9°$, corresponding to transect A, B, and C, respectively, in Fig. 1 of the main article) and 3 different granular mass densities (1700, 2000, and 2500 kg/m^3). Friction angles are fixed at $[10, 15, 10]°$, and m_f is fixed at 10^{-3} m^{-1}. Red dots and bars show the best-fit values and corresponding max–min ranges for $\alpha_{\log}$, whereas blue dots and bars show those for α_{ref}. Horizontal lines denote the best-fit constant values obtained from these coefficients and ranges (values reported in the legend)

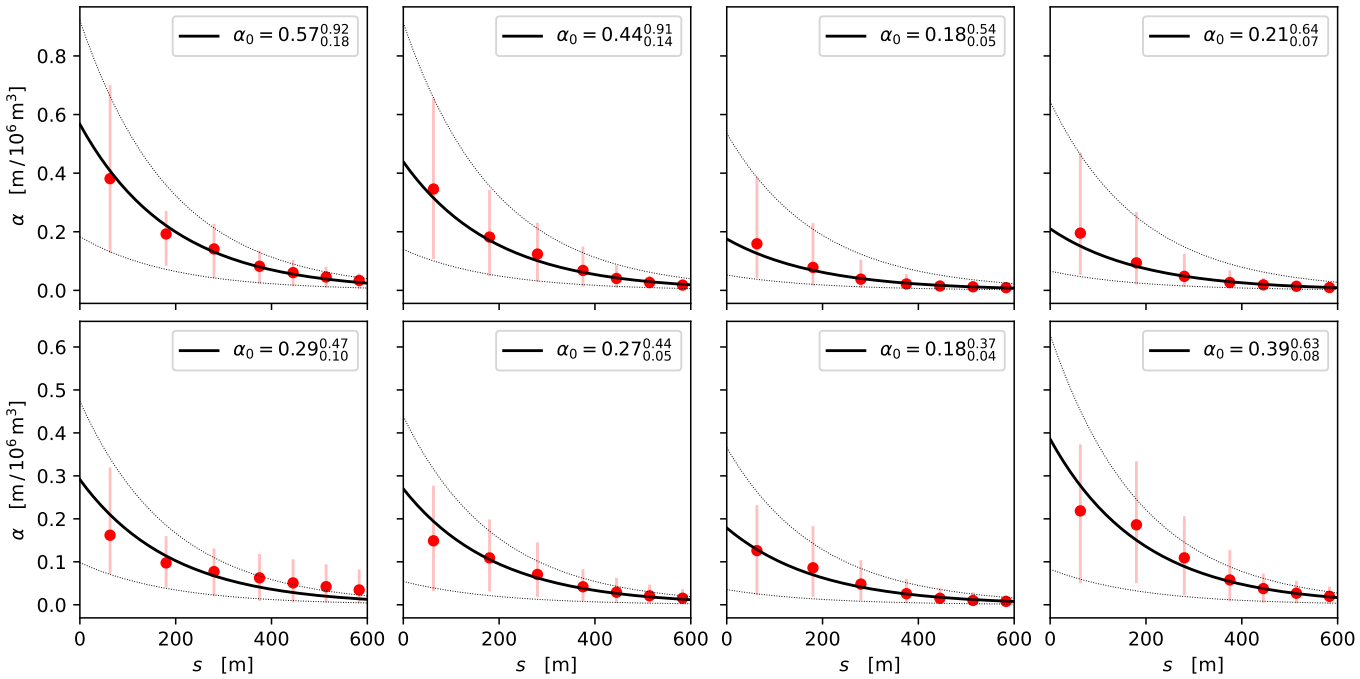

Figure S22. Dependence of the linear coefficient α on submergence depth s for submarine sources, for the extended dataset with landslide friction angles δ. The analysis includes 6 different configurations of friction angles ($\delta_1 = \delta_3 = \{5, 10, 15, 20, 25, 30\}^\circ$) and 3 different granular mass densities (1700, 2000, and 2500 kg/m^3). m_f is fixed at 10^{-3} m^{-1}, and D corresponds to transect B in Fig. 1 of the main article. Red dots denote best-fit coefficients; shaded red bars indicate the range between the maximum and minimum coefficients. Black curves are exponential fits (Eq. 4 in the main article), all with $s_0 = 191$ m. Legend entries give the values of α_0 as obtained by fitting central, maximum and minimum coefficients

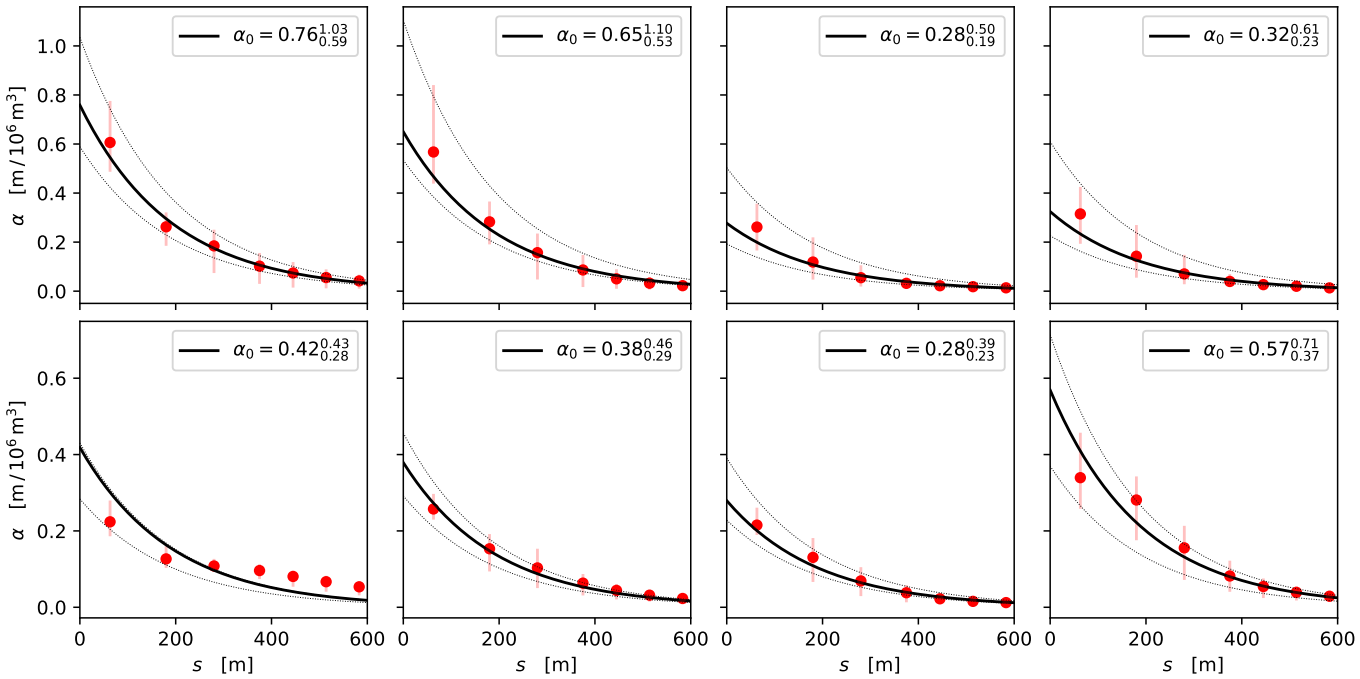

Figure S23. Dependence of the linear coefficient α on submergence depth s for submarine sources, for the extended dataset with landslide-water coupling m_f. The analysis includes 5 different values of m_f ($10^{-1}, 10^{-2}, 10^{-3}, 10^{-4}, 10^{-5}$ m^{-1}) and 3 different granular mass densities (1700, 2000, and 2500 kg/m^3). δ set is fixed at $[10, 15, 10]^\circ$, and D corresponds to transect B in Fig. 1 of the main article. Red dots denote best-fit coefficients; shaded red bars indicate the range between the maximum and minimum coefficients. Black curves are exponential fits (Eq. 4 in the main article), all with $s_0 = 191$ m. Legend entries give the values of α_0 as obtained by fitting central, maximum and minimum coefficients

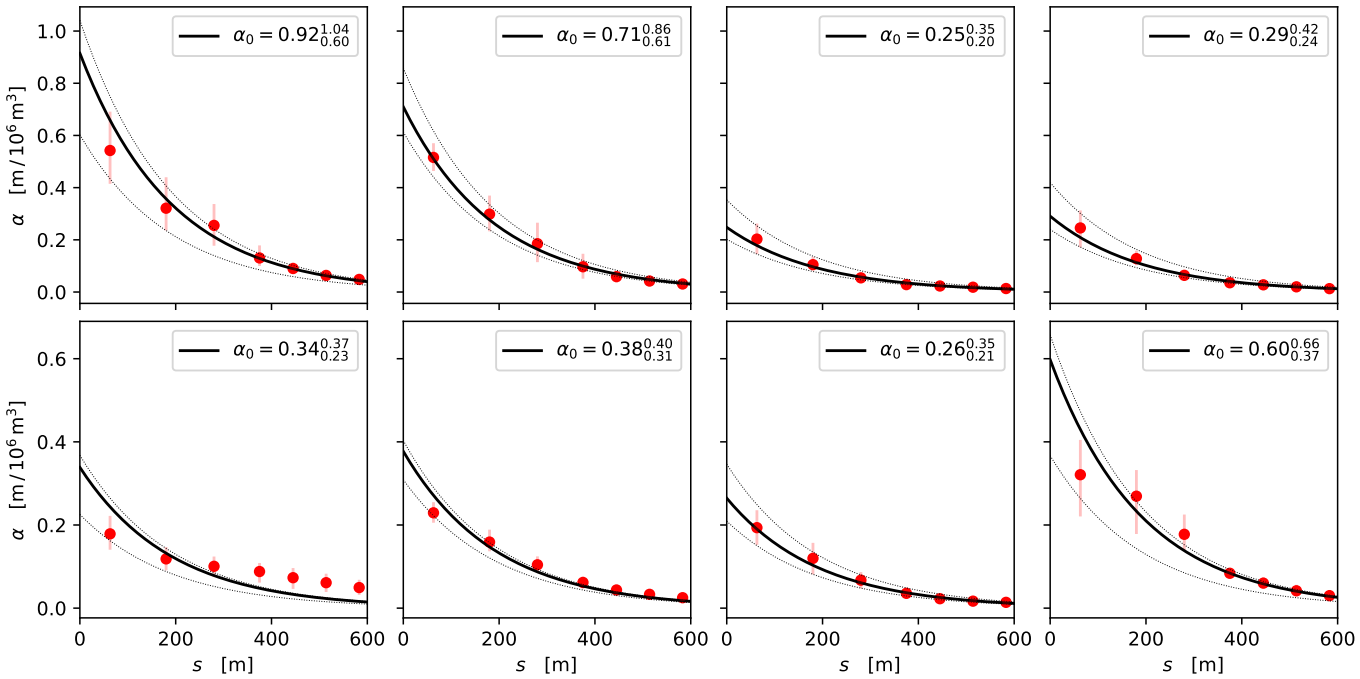

Figure S24. Dependence of the linear coefficient α on submergence depth s for submarine sources, for the extended dataset with source azimuth D. The analysis includes 3 different source azimuths $(312°, 320, 2°, 327.9°$, corresponding to transect A, B, and C, respectively, in Fig. 1 of the main article) and 3 different granular mass densities (1700, 2000, and 2500 kg/m^3). Friction angles are fixed at $[10, 15, 10]°$, and m_f is fixed at 10^{-3} m^{-1}. Red dots denote best-fit coefficients; shaded red bars indicate the range between the maximum and minimum coefficients. Black curves are exponential fits (Eq. 4 in the main article), all with $s_0 = 191$ m. Legend entries give the values of α_0 as obtained by fitting central, maximum and minimum coefficients

S5 Friction of the granular flow

A plot of the function $\mu(h_g, |\mathbf{u}_g|)$ is displayed in Fig. S25, when $\delta_1 = 10°$, $\delta_2 = 15°$, $\delta_3 = 10°$.

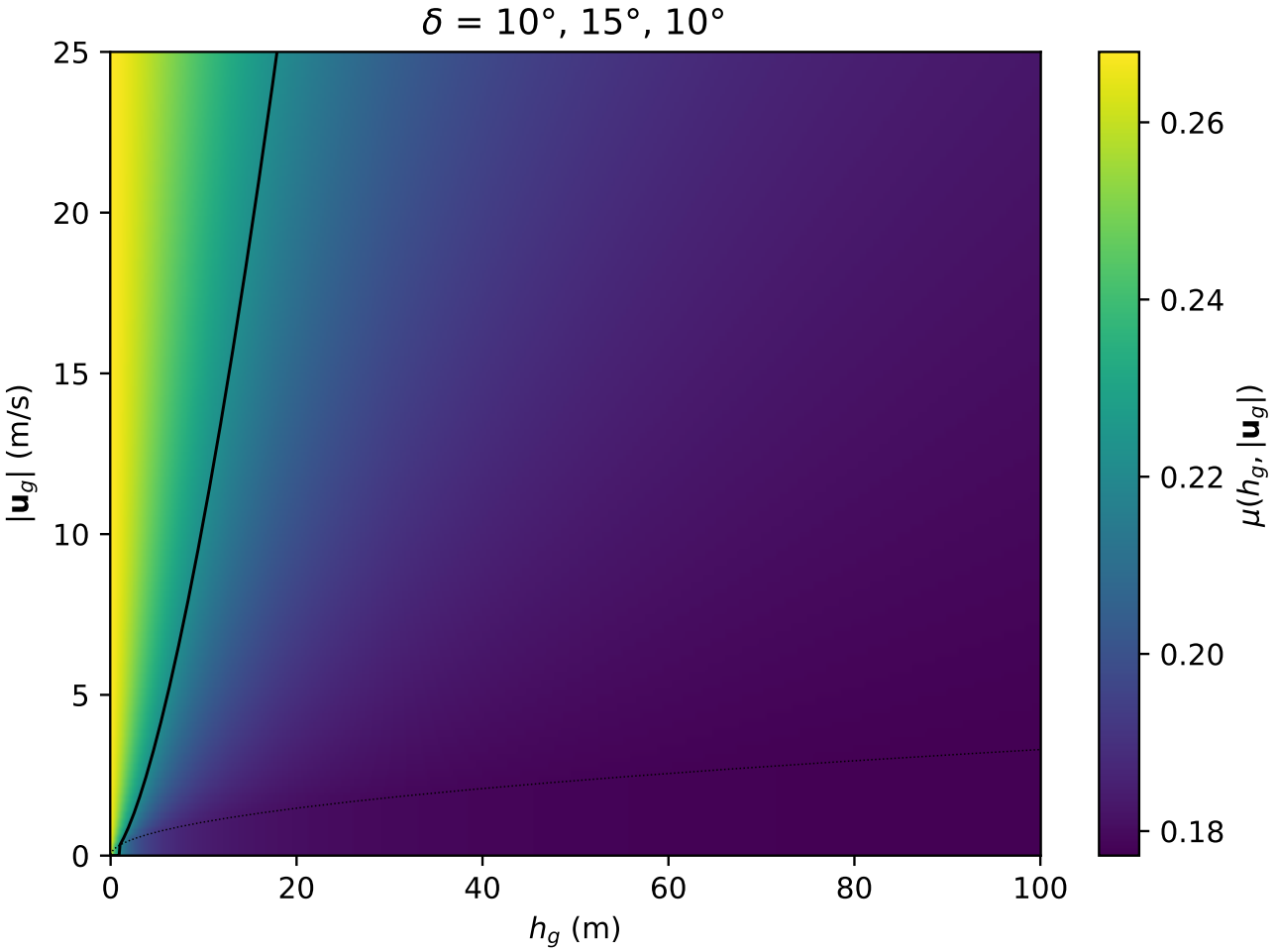

Figure S25. Pouliquenne-Forterre friction coefficient as a function of flow thickness h_g and velocity $|\mathbf{u}_g|$. The thick solid line highlights the transition between fast-thin ($\mu \simeq \tan\delta_2 \simeq 0.268$) and slow-thick flows ($\mu \simeq \tan\delta_1 \simeq 0.176$), see Eq. A5 in the main text. The thin dotted line marks the condition $Fr = \beta$